Molecular Imaging

and

Analysis of a fluorescence spectrum for determination of fluorophore depth

Master's Thesis
by
Khaled Terike and Daniel Bengtsson

Lund Reports on Atomic Physics, LRAP-XXX
Lund, January 2005

Abstract

In this study the goal was to map the field of molecular imaging and, especially, to find an optical method, within molecular imaging, to recover the distance of a simulated fluorescing lesion inside a tissue volume.

Spectral changes in the fluorescent light can be used to estimate the depth by measuring the fluorescence signal in different wavelength bands. By performing a ratio between the signals at two wavelengths we show that it is possible to determine the depth of the lesion. Simulations were performed and validated by measurements on a phantom in the wavelength range 815-930 nm. The depth of a fluorescing layer could be determined with 0.6 mm accuracy down to at least a depth of 10 mm.

Contents

1 Background and purpose

This thesis concerns the new, rapidly growing, biomedical field of research, Molecular Imaging. Our tasks are: (1) to describe Molecular Imaging in general to give insight to this new field of research in Lund. This study will mainly address the modality Optical Molecular Imaging. A part within this field will be given extra attention, the evolution of so called probes – molecules that are the core of the image signals. (2) The work also includes an important contribution to the research's central part, imaging. Within this area we will attempt to solve a problem within optical molecular imaging, to find a method which gives us depth information from the signal which is obtained when a probe is activated. This is amongst other things an important step towards eventually being able to reconstruct a tomographic image through molecular imaging.

The first part of the essay gives an inroduction to Molecular Imaging. What has emerged from the field along with potential fields of applications is described here. This section also treats the requirements for performing Molecular Imaging. The imaging modalities PET (Positron emission topography), SPECT (Single photon emission computed topography), MRI (Magnetic resonance imaging), CT (Computer topography) and ultrasound are not treated in any greater extent in this essay.

The next big section, Chapter 3, specifically treats optical molecular imaging. A more in-depth description of light emitting probes and how the signal is brought forth is given here. A couple of successful experiments within MI are also described in this chapter.
Chapter 4 concerns the interaction between light and tissue from a theoretical point of view as well as definitions of useful parameters within tissue optics. Finally, a description of the disposition and thought behind the experimental tests are given (Chapter 5 & 6) and later presented and discussed in Chapter 7 and 8.

The results of the completed experiments have been published in the article "Fluorescence spectra provide information on the depth of fluorescent lesions in tissue" which is found as an attachment to this essay.

2 Molecular Imaging

To explore things we cannot see with our own eyes has for long been of great interest to man. Through the history new imaging techniques have played an important role in the understanding of how our world is constructed and how it works. Imaging with x-rays has been revolutionary for making diagnosis within medicine. The telescope is another imaging tool, which really has broadened our horizon and given us pictures from parts of our world that were unexplored for long.

For biologists the study of the form and structure of organisms and its parts relies on observations with microscopes. Molecular imaging is a biomedical research discipline that extends such observations in the living body of a plant or animal to a more meaningful degree. The images reflect in vivo biologic processes at the cellular and molecular levels in their native environment.

Molecular imaging is a complex field that requires knowledge from many different research fields; Biology, chemistry, medicine, pharmacology, medical physics, mathematics and informatics are all necessary parts of this new imaging model. Recent developments of different image-capture techniques belong to the central core of molecular imaging. See figure 2.1 below.

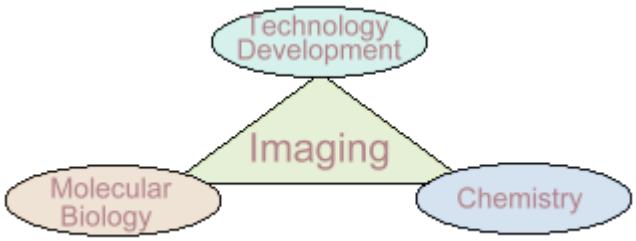

Figure 2.1. Molecular imaging is a multidisciplinary field that requires broad knowledge to conduct.

Present imaging technologies rely mostly on physiological or metabolic changes for distinguishing altered from normal tissue. With molecular imaging the focus is moved one step further; the molecular abnormalities that are the basis of the disease are investigated, rather than the end effects of such molecular alterations. This change from a non-specific to a specific approach describes an important progress where imaging can be used for better understanding of biology, for earlier detection of disease, and for evaluating treatment outcome.

Molecular imaging has emerged from recent advances in molecular and cell biology techniques, development of new imaging instrumentation such as positron emission topography (PET), magnetic resonance imaging (MRI) and optical imaging and the possibility of purposely transfer genes between organisms (especially to mice). Also, the availability of new contrast enhancing agents, that are highly specific, is a fundamental part within the field.

The goals possible to achieve in biomedical research, thanks to the development of molecular imaging are: (a) being able to study specific cellular and molecular processes taking place in the living body of an animal (*in vivo*), without involving entry (*noninvasively*); (b) to watch multiple molecular events that occurs within a short time; (c) to follow targeting or trafficking of cells; (d) to optimise drug therapy; (e) to image the effects different drugs have on molecular and cellular level; and (f) to evaluate and map disease progression at molecular level. Specifically, molecular imaging is considered to be an extraordinary opportunity for research in cancer[1].
Molecular imaging has its roots within nuclear medicine. Nuclear medicine is a discipline focused on labelling substances in the human body with radiotracers and in such manner follow and map those roles. In today's molecular imaging, the principle is the same but has been extended to other imaging modalities as well and consequently other sources for contrast than radiotracers. The imaging modalities that have been used until now are CT (computer topography), MR imaging (magnetic resonance imaging), nuclear imaging techniqes (PET, SPECT and gamma scintigraphy), nanosensors, optical imaging and ultra sound. The different imaging modalities are suitable for diverse purposes and the probes that are developed are designed according to which modality is to be used. In Ref 32 a number of gene products with corresponding suitable imaging technique are described.

The physicist role in molecular imaging is mainly the development and management of the advanced imaging technology used, but also in the interpretation of the captured signals and the reconstruction of clear and understandable images.

2.1 Advantages of molecular imaging strategies

In order for a physicist to understand the advantages molecular imaging provide it is important to be familiar with how biomedical research is pursued today and what limitations it faces. Along with some terminology this section will give some briefing on the subject.

The nucleus of the cell contains the genetic information of a human being. This information is kept in the chromosomes that are built up by DNA stands. Some of this information is used to express proteins. The proteins have many important functions in the body; structural and regulative among others. For a protein to be expressed the information in the DNA (genes) has to be encoded. The DNA is for this purpose transcribed into RNA - a new molecule that is a copy of the DNA. The RNA acts like a template for the proteins that are put together at the ribosomes.
If any of those steps goes wrong, undesired proteins will be formed, affecting the important functions they have. In cases when the body is unable to remove such mistakes they can give rise to disease[3].

Revolutionary with molecular imaging is that these proteins can be tracked and imaged. This is done by means of probes with a signal-emitting particle (e.g a fluorchrome or radioactive particle). By finding a protein that is expressed at a certain disease, it will be easier to develop drugs that stop those proteins from being effective. If cancer is caused by the defect gene the proteins can be imaged to follow its metastasis etc. Using protein tagging for mapping the *distribution* of an animals own proteins servers as another example of the potential this

method has. Mapping the distribution of proteins and enzymes can be used to track embryotic development in action – to see at exactly what point different enzymes get turned on in cells[4]. There are, however, further advantages of using highly specific probes. Imaging of proteins, enzymes and other biomolecules can be used to study the *genes* from which they emanate. This kind of research is referred to as gene expression studies. The answers scientists seek by studying gene expression are very profound; What function does a certain gene have? Did we manage to replace a defect gene successfully? Or; does a patient have genetic material that could be dangerous? Gene expression (figure 2.2) is best understood by describing how defect genes can be replaced (gene theraphy) and by decribing how a specific genes function is found out in present research[3].

To cure a defect gene, the damaged part of the DNA must be replaced with an intact replica. To produce this replica mRNA (messenger RNA) from a healthy cell is taken. In a laboratory this mRNA is transformed into complementary DNA (cDNA). This is done via an enzyme called reverse transcriptase. In the next step this cDNA is copied to DNA templates. The last step is to introduce the DNA into the defect cell and wait for the cell to begin expressing the new, undamaged, genetic information. Integrating the DNA into a delivery vehicle makes introduction of the DNA possible. The delivery vehicle, or vector, could for example be a virus[3].

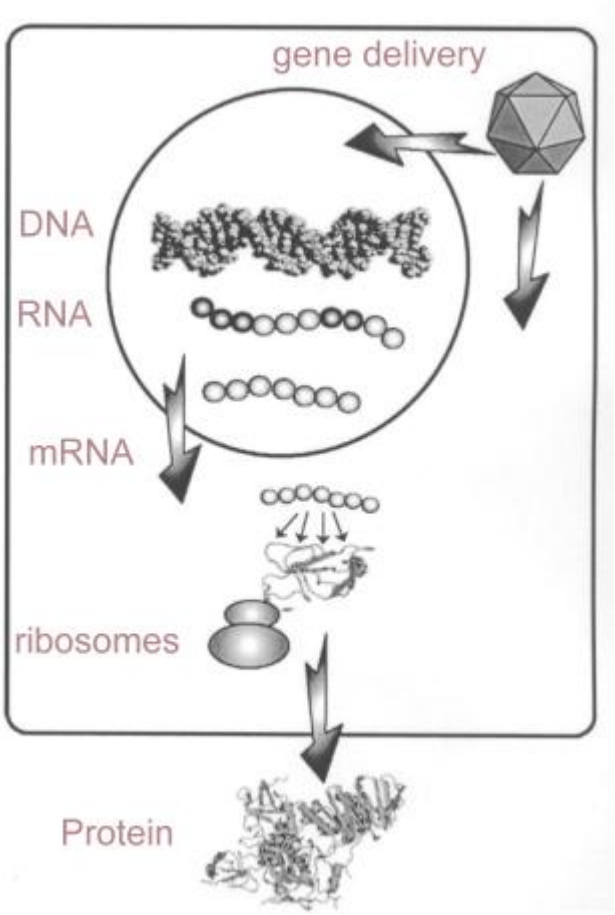

Figure 2.2. Gene expression. Process where the coded information in a gene is converted into many of the structures present and operating in the cell. Expressed genes are first transcribed into mRNA and then into proteins. Modified from Ref 3.

It is, however, not trivial to tell whether a gene has been replaced successfully or not. One could imagine the construction of a probe that tags and is activated by interaction of a protein coming out from the undamaged gene, but that is insensitive to proteins expressed from the damaged gene. In such manner a successful gene transfer could be tested. However, some proteins are more difficult to track than others, and this method implies a great deal of work since developing a new probe for each target (replaced gene) would be necessary. A complementary method is therefore often used. Along with the healthy, undamaged, DNA that is introduced in the cell, additional genetic material is included. The additional material is a so-called reporter or marker gene - a gene that encodes for an easily detectable protein. So, if the DNA is replaced successfully, a well-known detectable protein will also be expressed (figure 2.3). It is important for gene therapists to know what cells the gene is going into and where it is being expressed[4].
This method can not only be used for validating if a gene is successfully transferred. Also, it can be used generally to determine the patterns of gene expression that encode normal biological processes, or, by transferring genes that have unknown functions, to find out certain genes functions[3].

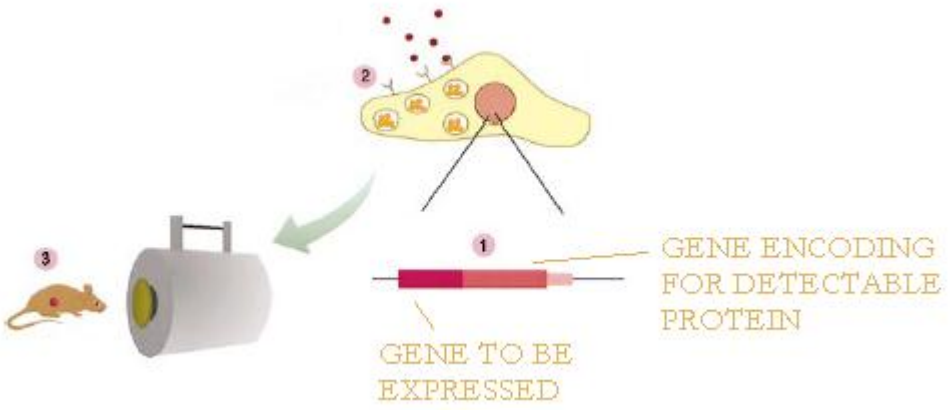

Figure 2.3. Along with the genetic material that is going to be expressed a reporter gene is delivered (1). If the delivery is successful an easily detectable protein is expressed that can be marked i.e. by a intravenously injected probe (2). The gene delivery can then be imaged (3).

Within molecular imaging there are two classes of marker genes that have been used for investigation: (a) marker genes encoding intracellular enzymes and (b) marker genes encoding cell-surface proteins or receptors. Intracellular expressed proteins has the advantage of being relatively invisible for the immune system whereas surface-expressed receptors are easier to detect since the probe not necessarily need to penetrate into the cell. Neuroscientists have used radio-labelled probes that bind to some types of receptors that are placed on the surface of nerve cells in the brain. In such manner they have managed to map nerve cells that use dopamine and serotonin[4].

Researchers are also looking for another technique that would have far broader applications: imaging the expression of native genes. The idea is to use probes that bind to mRNA-molecules. mRNA are the molecules that turn on the production of proteins in cells. This would help doctors to tell whether patients are expressing particular genes. By looking at reduced effect of the genes that enable cancer cells to multiply rapidly, doctors could measure the effectiveness of cancer therapy[4].

Some biotech companies have developed molecules that bind to mRNAs from such genes in order to block the production of the proteins they code[5].
The development of high-affinity probes and marker genes is a fundamental part of molecular imaging. It implies great progress within all types of biological research but what differs molecular imaging from conventional techniques is its applicability to living subjects.

Defining gene expression pathways is at present successfully done using conventional in vitro and cell culture techniques. Despite the success and rapid progress these conventional techniques have implied molecular imaging provide further advantages for these kinds of studies.
In many cases the outcome of a certain gene is not only dependent on the genotype, but also influenced by environmental factors. The predicted outcome of a gene, from in vitro studies, can be quite different when studied in a living animal[1]. In vivo molecular imaging provides the opportunity to study what effect those additional factors, such as physiological whole-body contributions of proteins, have in the biological pathways. The function and interaction of a specific gene becomes more realistic when studied in intact animals where the biological system is complete, and the complex biological network is not overlooked.

Molecular imaging in intact living animals can, as mentioned, also be of benefit within pharmaceutical research. In combination with transgenic animal models, the discovery of new drugs becomes easier. Because this kind of studies includes effects of transport/delivery, metabolism and excretion, new drugs can be excluded or accepted quicker than before. Molecular imaging facilitates validation of the target protein, evaluation of test compounds, studies of toxiological effects of the drug and testing its efficiency[1].

The possibility to perform repetitive studies of the same animal is a further advantage over in vitro and cell culture experimentation. The studies can be performed at different time points, with the same or with different molecular imaging modalities, all in the same animal. This gives a clearer vision of how biological parameters under examination change over time. This yields better results from fewer experimental animals.

Molecular imaging and standard use of conventional imaging can complement each other in a satisfying way. A good example of this is described by Bremer et al. (Ref 6). Here two equally sized tumours have been implanted in a mouse one which is more aggressive than the other one. With MRI the exact position and size of the tumours can be revealed but it does not provide any information about the aggressiveness. A probe designed to tag a protein which is only expressed in the more aggressive tumour is designed. The probe is fluorescent and reveals the difference between the tumours. If only molecular imaging would have been used just one of the two tumours would have been visible.

The ability to perform both tomographic imaging and quantitative measurements over time (four-dimentional information) could be possible with molecular imaging without being too time consuming. However, more research is required within this field.

2.2 Molecular imaging modalities and techniques

The development of new clinical imaging technologies has made rapid progress the last decade. The research has concentrated on changing focus from in vitro to in vivo imaging. Of special interest has been development of technology that allows non-invasive, high-resolution, small-animal imaging. Small systems are very useful when conducting laboratory studies within molecular imaging since they are relatively simple and inexpensive in contrast to the corresponding used for clinical purposes. However, an important issue and challenge within research on imaging technology is how to further expand this instrumentation and techniques so that it becomes applicable to human studies.

In small animal research one aims to obtain as high signal as possible with a high temporal resolution and with minimum amount of probe. The goal is ultimately to develop a single device that produces three-dimensional images of anatomical and biological information together. So far there is no such device but one must choose the most suitable for the experiments meant to be conducted. The characteristics that separate different instrumentation form each other are:

- resolution (spatial and temporal)
- depth penetration
- energy expended for image generation
  This depends on which component of the electromagnetic spectrum is utilized for generating images, i.e. ionizing such as CT (X-rays) and PET (γ-rays) or non-ionizing such as optical imaging (visible or NIR light) and MR (radio waves).
- whether there are injectable/biocompatible molecular probes available, and
- sensitivity of the system
  The sensitivity basically tells which the least detectable amount of probe is.

In table 1 below all available imaging modalities are mentioned with corresponding characteristics. Further discussion will not be conducted in this text but for more reading on the subject the internet page http://www.mi-central.org is recommended.

Table 2.1. Characteristics of imaging modalities available[1]

Imaging technique	Portion of EM radiation spectrum used in image generation	Spatial resolution	Depth	Temporal resolution	Sensitivity	Type of molecular probe	Amount of molecular probe used
Positron emission topography (PET)	high-energy γ rays	1-2 mm	no limit	10 sec to minutes	10^{-11}-10^{-12} mole/L	radiolabeled, direct or indirect	nanograms
Single photon emission computed topography (SPECT)	lower-energy γ rays	1-2 mm	no limit	minutes	10^{-10}-10^{-11} mole/L	radiolabeled, direct or indirect	nanograms
Optical biolumine-scence imaging	visible light	3-5 mm	1-2 cm	seconds to minutes	possibly 10^{-15}-10^{-17} mole/L	activable indirect	micrograms to milligrams
Optical fluore-scence imaging	visible light or near-infrared	2-3mm	~1cm	seconds to minutes	likely 10^{-9}-10^{-12} mole/L	activable direct or indirect	micrograms to milligrams
Magnetic resonance imaging (MRI)	radiowaves	25-100 μm	no limit	minutes to hours	10^{-3}-10^{-5} mole/L	activable direct or indirect	micrograms to milligrams
Computer topography (CT)	X-rays	50-200 μm	no limit	minutes	not well charachterized	may be possible	not applicable
Ultrasound	high-frequncy sound	50 - 500 μm	millimeters to centimeters	seconds to minutes	not well charachterized	limited activable, direct	micrograms to milligrams

Imaging technique	Quantit-ative degree	Ability to scale to human imaging	Principal use	Advantages	Dis-advantages	Cost
Positron emission topography (PET)	+++	yes	metabolic, reporter/gene expression, receptor/ligand, enzyme targeting	high sensitivity, isotopes can substitute naturally occurring atoms, quantitative translational research	PET cyclotron or generator needed, relatively low spatial resolution, radiation to subject	****
Single photon emission computed topography (SPECT)	++	yes	reporter/gene expression, receptor/ligand	Many molecular probes avaliable, can image multiple probes simultane-ously, may be adapted to clinical imaging systems	relatively low spatial resolution because of sensitivity, collimation, radiation	***
Optical biolumine-scence imaging	+ to ++	yes but limited	reporter/gene expression, cell trafficking	highest sesitivity, quick, easy, low-cost, relative high-throughput	low spatial resolution, current 2D imaging only, relatively surface-weighted, limited translational research	**
Optical fluore-scence imaging	+ to ++	yes but limited	reporter/gene expression, cell trafficking	high sesitivity, detects fluorochrome in live and dead cells	relatively low spatial resolution, surface-weighted	*-**
Magnetic resonance imaging (MRI)	++	yes	morphological reporter/gene expression, receptor/ligand if many receptors	highest spatial resolution, combines morphological and functional imaging	relatively low sensitivity, long scan and postprocessing time, mass quanty of probe may be needed	****
Computer topography (CT)	not applicable	yes	morphological	bone and tumor imaging, anatomical imaging	limited "molecular" applications, limited soft tissue resolution, radiation	**
Ultrasound	+	yes	morphological	real-time, low cost	limited spatial resolution, mostly morphological	**

2.3 Requirements for performing molecular imaging

Analyzing tissue samples ex vivo is relatively easy compared to corresponding studies conducted in living subjects. Ex vivo studies are done using test tubes that contain cell extracts or intact, cultured, living cells. Different cellular processes can be tested by means of reagents added closely to the cells or even injected into the proper cell. To image specific molecules in vivo is more of a challenge. Several criteria must be met after an appropriate target has been selected:

- A molecular imaging probe must be developed. The task of the probe is to distinguish the particular biological process and help to generate images of the target. The probes must have the right chemical, biochemical and molecular properties to manage this in vivo.
- The probe must posses the ability to overcome biologic delivery barriers. Such barriers could be the cell membrane, of interstitial[a] or vascular[b] nature.
- An amplification strategy must be used so that the concentration of the probe is sufficiently large after interaction of the target.
- Sensitive, fast, high-resolution imaging techniques must be available.

2.3.1 Probes

Molecular probes provide the signal in almost all molecular-imaging assays. The only exception is MRS, which is a spectroscopic method for analysing tissue. MRS belongs to the same family as Magnetic resonance imaging (MRI). The signals constitute the spectra which emanate directly from the molecules in the tissue under examination.

Probes used for molecular imaging are injected into the living subjects to image specific molecular and biological events. A probe typically consists of two components coupled together; one that interacts with the target and one that emits a signal. The interacting component should have as high affinity as possible to the target so that the probe accumulates in large amounts where the target is present and exclusively in these regions. This component is often referred to as delivery vehicle. The signalling component is for tracking the probe so that the target can be imaged. The nature of the signalling component depends on which device is used for capturing the signal. In radio labelled approaches it is often a single atom with radioactive properties (such as $^{11}C, ^{18}F$ or ^{99m}Tc) that is attached to the delivery vehicle whereas in optical approaches fluorescent molecules (fluorochromes) are used. For MRI the signalling component is some kind of paramagnetic atom[1].

Probes can be categorized as radio labelled or activable probes. Radioactive probes (for PET and SPECT imaging) produce a signal continuously, before and after interacting with their target. Activable probes emit a signal only after interaction with the target and are undetectable before. These probes are used for optical imaging among others. This is a broad categorization that covers most available probes and some further classification could be

[a] Interstitial - Characteristic of a particular organ or tissue.

[b] Vascular - Relating to a channel for a body fluid; especially blood vessels.

useful. Due to difficulties for the probes to reach their targets (see section 2.3.2) some probes are less direct than others. Instead of interacting directly with the target, indirect probes are made to image substances associated with expression of the target.

Molecular imaging probes can be small molecules such as receptor ligands[c] or enzyme substrates[d], or higher-weight affinity ligands (figure 2.4). Examples of the latter are monoclonal antibodies and recombinant proteins. Monoclonal antibodies are proteins with a definite structure that binds antigens[e] and are made by cell culture technique. Recombinant proteins are genetically engineered proteins[7].

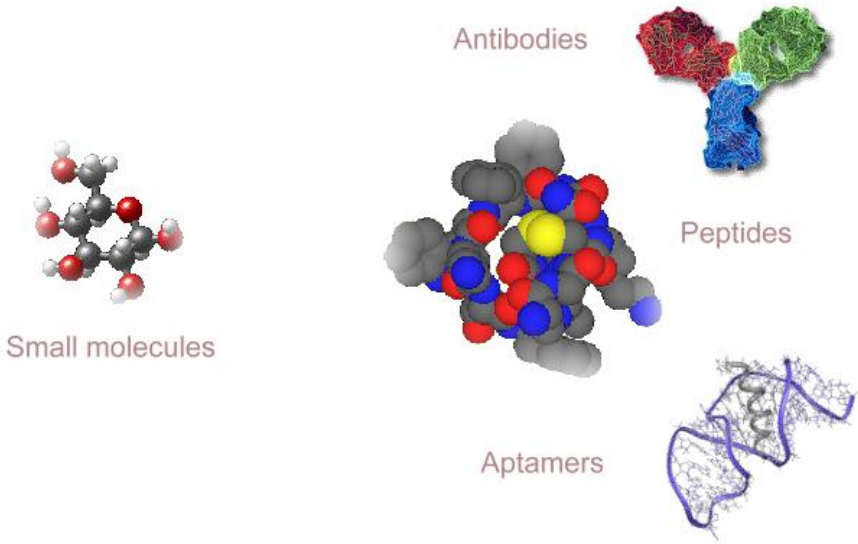

Figure 2.4 (Modified from Ref 7). Biological molecules for targeting/imaging. Higher-weight affinity ligands such as antibodies (proteins), peptides (molecule composed of up to 20 amino acid residues joined by peptide bounds) and aptamers (nucleic acids) are suitable delivery vehicles for molecular imaging probes. Small molecules (~300u) are characterized by high specificity, high affinity binding to receptors, transporters or enzymes and rapid distribution/clearance (minutes/hours). Heavier molecules (antibodies ~150 000u) have high affinity to a variety of targets and slow distribution/clearance (days/weeks).

The most common type of probes are the non-specific with vascular distribution, e.g., circulating within blood vessels. Most of the contrast media in conventional medical imaging is of this kind, but they are also being used in radionuclide and optical imaging. Indocyanine green is a widely used fluorescent contrast agent that belongs to this group. They can be used to image physiological processes such as flow and changes in blood volume but cannot image specific biological processes at cellular or sub-cellular level. Still they are useful for studying "downstream" changes in disease process although not suited for monitoring the very early alterations[8].

For better targeting potential, probes can be made using substrates that can interact with targets within cells or with separate sub-cellular sections. For this purpose antibodies or

[c]ligands are used. These kinds of probes are the second most common and are mainly used for radionucleic and optical imaging. The probes can be used to image the end products of gene expression by letting the probe interact with the original protein expressed from a specific gene. The limitation of this approach is the rather difficult and expensive development of these probes. For each new protein to be targeted a new substrate must be discovered and radio-labelled. It is desirable to discover a method that could image gene products from any gene of interest and many research groups have put effort in putting reporter gene/reporter probe systems together in order to decrease the amount of work for this kind of research[1].

The probes mentioned above have one major drawback: background noise can disturb the measurements with such probes. The first mentioned type of probes, the non-specific with vascular distribution, give rise to a signal independently of where in the living body the probe is, even in their activable mode (i.e indocyanine green). Neither, for the second kind of probes, can a bound probe be distinguished from one which has interacted with its target. In order to bypass this, other probes have been developed. Probes with these characteristics are especially so-called smart probes and optical reporters. These probes are especially suitable for optical imaging and will be discussed under sections 3.1.3 and 3.2.1.

2.3.2 Overcoming deliver barriers

Molecular imaging probes face many obstacles well inside the body. In order to reach the target in sufficient concentration and to stay there long enough it has to avoid being transported away, fragmentation and overcome delivery barriers. Overcoming delivery barriers is the most challenging and several strategies have been developed to make this possible. The probe could be made more "invisible" for the body by decreasing its sensitivity to immune response, which gives it more time to reach the target without being carried away or recognised immediately. At the cell surface mechanisms that shuttles the probe into the cell can be utilised. Smart probes are often made long circulating in order to achieve a more homogeneous distribution. Long circulating times are usually not desirable, but smart probes are built up from a main structure (copolymer chain) that helps the probe to reach cells by slowly passing from the blood vessels into the surrounding tissue[9]. Local delivery is another way of bypassing delivery barriers.

2.3.3 Amplification strategies

In molecular imaging the amount of targets can be very limited, and it is important that the signal from the probe is as strong as possible. A signal emanating from deep inside a body faces many obstacles, preventing it from reaching the detector. To deal with this problem different amplification strategies can be used. When possible, as many signal emitting particles per probe is one way to facilitate detection. This strategy is used for smart probes that are described in section 3.1.3 along with a successful example of molecular imaging. To choose targets carefully is another way of minimizing this problem. For instance, if the intention is to visualize a cancer tumor it is appropriate to choose a target that is not only associated with the tumour but also expressed in

[c] Ligand - For a single larger molecule or receptor site, any of the smaller molecules or ions that are able to bind with the larger molecule or site.
[d] Enzyme - Biologic macromolecule that acts as a catalyst by lowering the activation energy of a reaction. Enzymes are proteins or RNAs. A substance that an enzyme acts upon is an enzyme substrate.
[e] Antigen - Any material that is dissimilar to structures in an organism and is recognized and bound by an antibody

large amounts. Imaging with proteins as targets do not require amplification in the same extent as for example RNA targeted imaging would do, since the amount of RNAs per cell is much less.

3 Optical imaging

Optical techniques for imaging rely on the use of electromagnetic radiation in the visible to infrared wavelength range to reconstruct images. Whereas in MRI or PET paramagnetic and radioisotopes are used for tracing the probes, optical imaging probes are supplied with a light-emitting marker (fluorochrome). When interacting with the target such probe acts like a bright spot in a dark surrounding. The use of non-ionizing radiation as signal source makes optical imaging a harmless method to use for medical and biological purpose.

Optical molecular imaging techniques can be subdivided into two groups: fluorescence imaging (figure 3.1) and bioluminescence imaging (figure 3.2). The classification depends on how the remitted signal is brought forth: (1) *fluorescent* markers require an external source of light for excitation and emit light at a different wavelength for detection, and (2) *bioluminescent* markers do not need any external excitation light source. As the names suggest this is from where the optical imaging techniques *fluorescence-* and *bioluminescence imaging* origin.

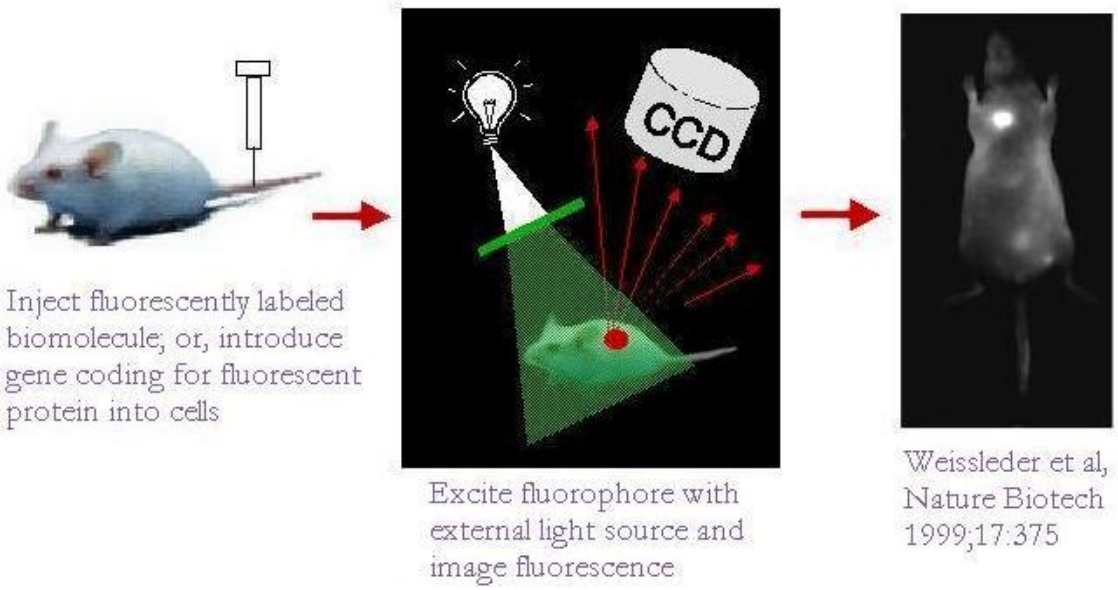

Figure 3.1. Fluorescence imaging. Reprinted from Ref. 7.

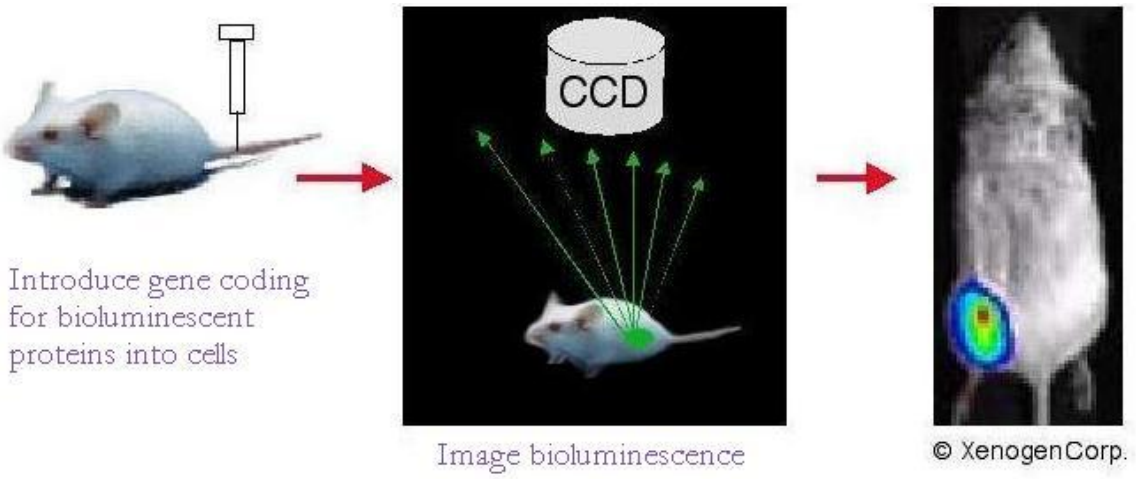

Figure 3.2. Bioluminescence imaging. From Ref 7.

In section 2.1 two approaches for imaging were described: one (gene delivery) where the cells were modified with extra genetic material that give rise to enzymes or proteins (intracellular enzymes or cell-surface proteins or receptors) that could be traced and detected by probes (figure 2.3), and another, where probes were developed to trace natural proteins, i.e. proteins expressed in the body from non-modified genes. Optical molecular imaging provides a slightly different approach for gene expression studies. Instead of delivering genetic material and then inject probes to detect the outcome of these delivered genes (reporter genes) optical molecular imaging fuses these two steps into one. The genetic material delivered encodes for proteins that are light-emitting themselves, so that no other probe has to be added. The genetic material is naturally occurring and can be found in algae's and butterflies among others. These types of genes are called optical reporter genes. They can encode for fluorescent as well as bioluminescent material. Fluorescent molecules can also be used in an "ordinary" manner – attached to a bio molecule that interacts with a protein in the body. This sums up the existing options of using light-emitting markers for molecular imaging (figure 3.3).

Figure 3.3. Optical reporter genes can be used within both fluorescence imaging and bioluminescence imaging. Fluorescent molecules can also be used as exogenous probes when tagged to bio molecules.

An essential issue in optical imaging is how to detect the emitted signal from the probes. The most commonly used detectors are the charged coupled device cameras (CCDs). CCDs have high sensitivity, good linear response and cover a wide range of wavelengths. A CCD can, leaving detailed explanations out, be described as a semiconductor chip with one face sensitive to light. The light sensitive face is rectangular and subdivided into a grid of discrete rectangular pixels, each about 10-30 micron across. A photon hitting a pixel generates a small electrical charge which is stored for later read-out. The more photons hitting a pixel the greater gets the charge. An image is reconstructed by estimating the amount of light that has

struck each pixel. CCD cameras have many application fields, not only within research but also commercially. Due to the high availability and simple construction of the detector, optical imaging is far cheaper than the other imaging modalities (such as MRI, PET, SPECT etc) listed in table 2.1 (section 2.2). One important drawback with CCD cameras is that it is difficult to image anything but small areas. The size of the chip is limited because of the time required to read it out. In laboratories, optical fluorescent- and bioluminescent imaging using CCD cameras have successfully been used for studies of physiological events in mice. However, for human studies the applicability is far more limited. Further, images obtained with a CCD camera are two-dimensional and lack depth information. This information is essential for volumetric (tree-dimensional) imaging.

3.1 Fluorescence imaging

Fluorescence is emitted when a fluorophore (also called fluorochrome or fluorescent dye) interacts with an incident photon. A photon absorbed by the fluorophore causes an electron in the molecule to rise from its ground state to a higher energy level. This is called excitation of a fluorophore. When the electron reverts to its original level, a photon is released - a phenomena referred to as fluorescence emission. Due to energy dissipation (to vibration levels, thermal energy etc.) during the time the fluorophore is in its excited state, the energy of the released photon, $h\nu_F$, is lower than the excitation photon, $h\nu_{ex}$. This process is represented by the Jablonski diagram (figure 3.4).

The ground state of a fluorophore is actually not discrete but consists of many nearby energy levels. When incident photons are absorbed by fluorophores the emitted light is made up by a lot of different wavelengths because of these different possibilities of relaxation. The excited states - S_1 and S_2 - also consist of several levels. The result of this is that the electronic transitions $h\nu_A$ and $h\nu_F$ are broad energy spectra called the fluorescence excitation and fluorescence emission spectrum (figure 3.5).

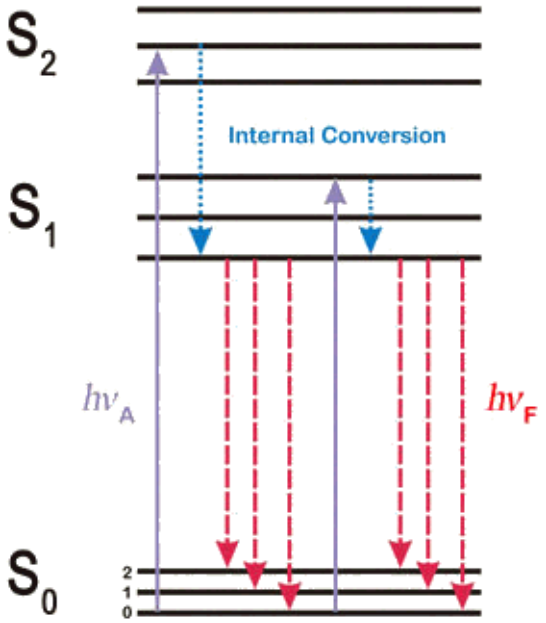

Figure 3.4. A generalized Jablonski diagram. A photon with a frequency of ν and energy of $h\nu_A$ is absorbed by the fluorophore. Some of the energy is lost and usually puts the fluorophore in the lowest excited energy state S_1. The fluorophore then returns to the ground state by emission of a photon with energy $h\nu_F$, which varies depending on what S_0 ground-state level it returns to. Reprinted from Ref 10.

There are various ways fluorescence can provide information in imaging[11]. For example: (a) an imaging system can be tuned to cover a fluorophores emission spectrum; which makes it possible to localize the fluorophore. For example, cells expressing green fluorescent protein can be imaged and counted after reporter gene delivery. (b) When a fluorescent molecule is changed in any sense (such as binding of ions in the body, changes in pH etc) the emission spectrum can alter as well. An imaging system able to detect such variations can be used to measure changes of the environment of the fluorophore. Methods for this kind of measurements have been developed for cellular and sub-cellular level. (c) Intensity measurements can be used to estimate the concentration of a fluorescently labelled bio molecule. It is possible to determine the presence of molecules, such as enzymes, proteins, DNA or antibodies, in very low concentrations, down to single molecules.

3.1.1 Major factors affecting the fluorophore performance

As mentioned in the introduction to this chapter fluorescent probes can either be made of a fluorophore coupled to a biomolecule, or, consist of genetic material that, well inside the cell, encodes for a fluorescent protein. In the latter case there are few probes available. The genetic material comes from animals or plants and is very difficult to manipulate in order to e.g. change the spectral properties of the fluorescence light. Fluorophores coupled to bio molecules leaves much more options for the constructor. Thousands of fluorophores are available commercially and still many research groups choose to develop their own dyes. Several values are important to take into account when choosing a fluorescent dye for an experiment. Among others are:

- The dye's molar extinction coefficient (ϵ)
- Excitation wavelength
- Emission wavelength
- The fluorescence quantum yield of the dye (QY)
- The photostability of the dye
- The environment of the dye

The fluorescence output of a given dye depends on how efficiently it absorbs and emits photons, and how well it can handle repeated excitation/emission cycles. The molar extinction coefficient measures the dye's ability to absorb light. The value of ϵ is specified at a single wavelength, usually the absorption maximum. Most fluorophores in common use have molar extinction coefficients at their wavelength of maximal absorption ranging between 5000 and 200,000 $cm^{-1}M^{-1}$ (Ref. 10). The Stokes shift is the difference in wavelength between the fluorescence excitation maximum and the fluorescence emission maximum. In general, dyes with large Stokes shifts tend to have small extinction coefficients and dyes with small Stokes shifts tend to have relatively large extinction coefficients.

The excitation wavelength is where maximum absorption occurs. Normally, the excitation band is relatively broad (up to ±50nm on each side of the excitation wavelength)[12]. The shape of the emission spectrum does not change if the fluorophore is excited at another wavelength than where maximum absorption occurs, but the intensity of the emitted light is dependent of the amount of light absorbed. This is illustrated in figure 3.5.

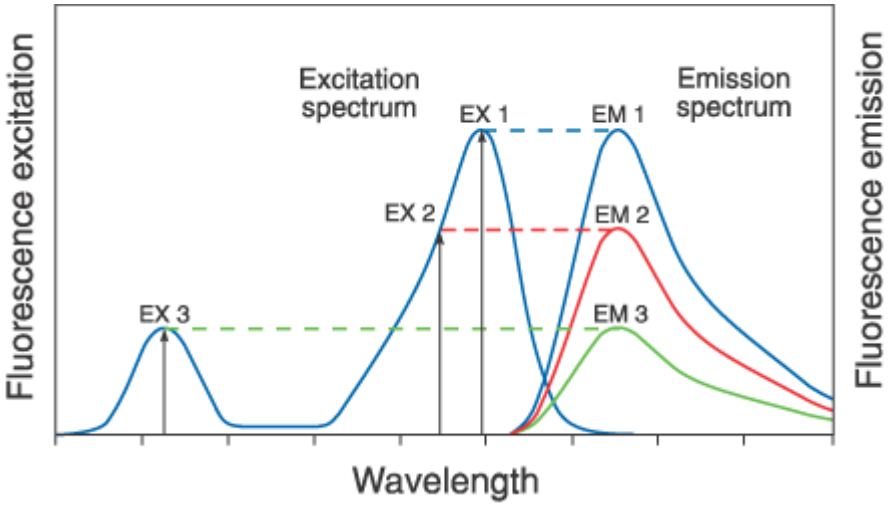

Figure 3.5. Typical excitation spectrum for a fluorophore. Three excitation wavelengths (EX1, EX2 and EX3) are shown with corresponding emission spectra (fluorescence spectra). Note that the shape of the fluorescent spectra does not change for the three excitations, but the intensity does. (From Ref 20)

The emission wavelength is the wavelength where the fluorescence light peaks. All light absorbed is generally not emitted as fluorescence light. Between absorption and fluorescence emission the fluorophore is in its excited state. During this time (~1-10 nanoseconds) the molecule is exposed to several possible interactions with its environment, and therefore decreases the possibility of fluorescence emission to occur. The fluorescence quantum yield is measures the efficiency with which the excited molecule is able to convert absorbed light to emitted light. It is defined as the portion of absorbed photons that are converted to emitted fluorescence photons. The quantum yield of most fluorophores varies between 0.05 and 1 (QY=1 means that every single photon absorbed results in emitted fluorescence). The quantum yield of most dyes decreases when they are coupled to proteins. It is also very sensitive to changes in pH and the temperature of the environment.

Photostability is a measure of how well the dye repeatedly can be excited and fluoresce without being destroyed. When a fluorophore is destroyed it is called photobleaching. This phenomenon normally only occurs when the illumination is very high and results in decreased ability to be detected.

The environment of the fluorophore can affect its performance. The effect can be favourable or undesired depending on the experiment. Binding to DNA or proteins, pH and the presence of quenchers are all factors that can change the fluorescence quantum yield of a fluorophore. The way the fluorophore affects its environment is another important issue to consider. The probe should not disturb the function of the cell or target molecule because of its size or non-desired binding.

In summary, a fluorescent molecule used for molecular imaging should have high quantum yield, high extinction coefficient at the excitation wavelength and high chemical- and photostability and not being toxic. In addition to this the fluorophore must be easily soluble in water. In many cases, however, changes can be made to the molecular structure to fulfill this requirement.

When it comes to synthesis probes for molecular optical imaging it is essential that fluorophore and the bio molecule can bind. The chemistry of fluorescent probes or fluorophores will not be discussed here; still some guidelines are worth to be mentioned. There are two major groups that separate fluorophores: amine reactive and thiol reactive. Amine-reactive probes are widely used to modify proteins, peptides, ligands and other biomolecules. Thiol-reactive reagents, on the other hand, are most frequently used to probe protein structure and function. This can be useful to know since the fluorophores offered commercially, for biomedical use (such as Molecular Probes, Inc.), often are grouped after their reactive groups. The large amount of avaliable fluorescent probes and application fields can namely be somewhat confusing.

3.1.2 Advantages of the near infrared (NIR) spectral region

The red region of the spectrum is appropriate to use from many point of views. Here, inexpensive and compact excitation sources are available, e.g. the He-Ne-Laser or laser diodes. Of more crucial importance, however, is the fact that light in this spectral range is less scattered and absorbed by biological tissue. This implies greater penetration depth of the light and clearer images. Biological tissue has a low degree of intrinsic (inherent) fluorescence in this range as well[8], so that the background is lower. However, not very many fluorochromes in the NIR region are available. This is due to some general problems with the syntesis of NIR fluorphores compared to visible light fluorophores[13], namely:

- As the wavelenght increases the spectrum is broadened.
- The quantum yield is lower
- The fluorochromes are less photostable
- Increasing red-shift leads to chemical instability, and
- They tend to aggregate because of poor water solubility.

One focus of research is therefore the development of dyes that fluoresce well in the region above 600 nm[13].

3.1.3 Probes for fluorescence imaging

Molecular optical imaging has an advantage over other imaging modalities through the different ways the probes can be constructed. For no other modaliy, genetic material that codes for signal-emitting substances is available. Fluorophores that are tagged to bio molecules are also different from their equivalents in other modalities. They can be made invisible until reacting with their target. This implies a large reduction of undesired background noise.

Smart probes, or beacons, are activable probes that can only be detected once they have interacted with their targets. They can be used both for in vitro studies and in living animals. The traditionally designed molecular beacon consists of a DNA strand. In one end of the strand a fluorophore is attached and in the other a quencher (figure 3.6). The DNA strand is then folded into a U-shape which puts the quencher and the fluorphore close to each other. Quenching is a bio molecular process that reduces the fluorescent quantum yield and prevents it from fluorescing. This can occur when one fluorophore is in close proximity to another, co called self quenching. When the probe hybridizes to DNA or RNA, the U-shaped stem is

unfolded and the two ends separated. The fluorophore is unquenched, allowing it to transfer energy by fluorescence resonance energy transfer (FRET). The probe lights up only when the reaction of interest has occurred. Such molecular beacons have been used to image a particular mRNA in leukaemia cells[14].

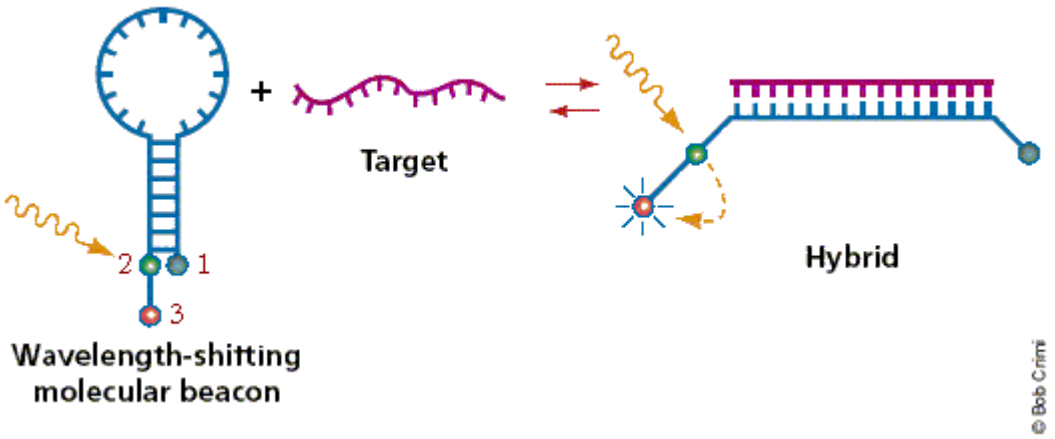

Figure 3.6 (Ref. 14). A conventional molecular beacon. The beacon is relatively insensitive to incoming light before interacting with its target. After interaction the quencher (2) and fluorophore (1) are separated. Energy absorbed by the fluorophore is transferred to the emitter (3), allowing detection.

A variant of these probes are the quenched near-infrared fluorochromes. These are smart probes that can be activated by so called proteases. The description of these probes along with clinical test results will serve as an excellent example of successful molecular imaging. Protease is when a protein is cleaved. This cleavage is catalyzed by enzymes. Depending on which protein is to be cleaved and which enzyme is involved in the process, those proteases have been given different names. In cancer progression proteases are key factors. One specific protease, cathepsine-B, correlates with tumors tendency to invade healthy tissue. In breast cancer, specifically, high levels of cathepsin-B have been linked to highly aggressive tumors. Bremer et al (Ref. 15) have developed a quenched near-infrared fluorescent probe that is turned on by cathepsine-B protease. The probe consists of a long chain of identical molecules with fluorophores coupled to it. Coupled to this structure are substances that cathepsine-B acts upon.

The fluorophores are put so close to eachother that self quenching occurs. The idea is to let the protease act upon the probe and when the probe is cleaved the quenching ceases. Two different types of breast tumors were implanted in a mouse, one with higher grade of invasiveness than the other. The tumors were small (sub millimeter) and of equal size. 24 hrs after injection (intravenously) of the probe, NIRF imaging was conducted (figure 3.7). The fluorescent probe reveals Cathepsine-B activity which makes the two small tumors visible. It is also obvious that in the highly invasive tumor (to the left in figure 3.7 A-C) this activity is higher.

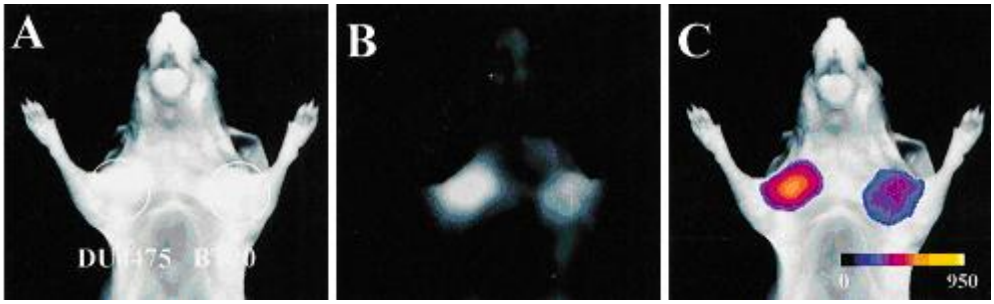

Figure 3.7. Reprinted from Ref 15. A. Light image, nothing revealing the tumors. B. Raw NIR image. C. Color encoded NIRF signal. The highly invasive breast tumor is the left one in the picture. The fluorescence is higher in the more invasive of the tumors.

First of all, the results serve as a demonstration of how molecular specificity of the fluorescent probes can be utilized in contrast to developing new optical imaging devices. Secondly, different levels of protease activity can be determined with NIRF optical imaging. Imaging of molecules such as those proteases may be used for earlier tumor detection. Also, imaging of proteases may be helpful for the treatment of cancer. More aggressive treatment could be appropriate for tumors with higher protease levels, while tumors with less may be treated more cautious.

Another possibility to extract molecular information in living subjects is to use fluorescent proteins by delivering fluorescent reporter genes to cells. Green fluorescent protein (GFP) is a protein from the jellyfish *Aequorea Victoria* that has been used for in vivo imaging. A drawback with GFP is the low emission wavelength (509 nm) which limits imaging with GFP to the surface of a body and also interferes with the autofluorescence of many tissues. There are mutants of GFP that has been engineered but the maximum wavelength-shift is only around 25 nm.

Genes encoding for red proteins have more recently become available. DsRed and HcRed fluoresces at 583 nm and 618 nm respectively. HcRed is especially suited for in vivo imaging and has been developed through mutagenesis of a non fluorescent protein from the coral *Heteractis crispa.* The main applications of fluorescent proteins is in monitoring tumor growth and metastasis formation, but has also been used in gene expression studies[16].
Quantum dots are a relatively new family of fluorescent probes that have many interesting properties. Quantum dots are non-organic fluororescent particles that are made of semi conducting materials. They are spherical in shape with a semiconductor nanocrystal core and a semiconductor shell protected by a polymer coat (figure 3.8). Antibodies or ligands for enzymes or receptors can be conjugated to the quantum dots similar to organic fluorescent probes. The particle absorbs light at a wide range of wavelengths but emits almost monochromatic light; which's wavelength only depends on the size of the particle. The fluorescence is much brighter than fluorescence from an organic molecule. Quantum dots are very stable in organic environments and their coating makes them less toxic than organic dyes. However, quantum dots are not smart, i.e. they fluoresce regardless of however they are bound or not. The first produced quantum dot applied to a living organism, a frog embryo, were reported as late as 2002[18]. Few other examples of quantum dots used in molecular imaging experiments are reported, but it is predicted to be among the most promising emerging fluorescent labels for cellular imaging in vivo[14].

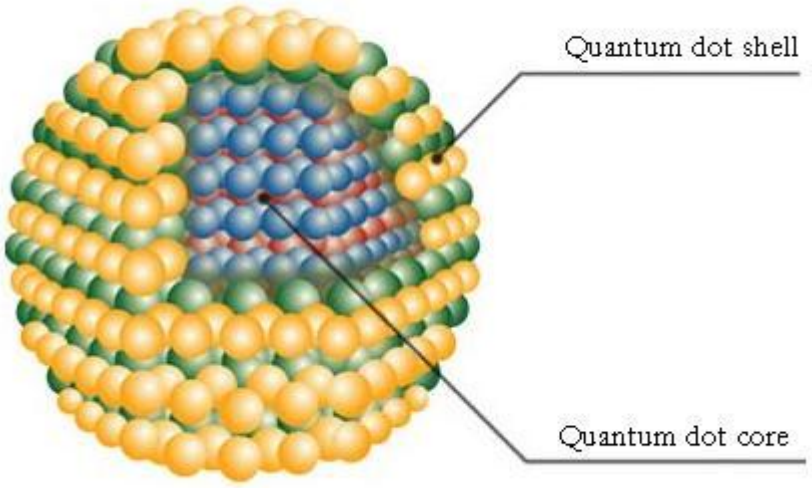

Figure 3.8. (Modified from Ref 17). The spherical shape of a quantum dot.

3.2 Bioluminescence imaging

Bioluminescence imaging is an optical imaging technique that makes use of energy dependent reactions as source for light emission, in contrast to fluorescence imaging, where light emission is stimulated by absorbed photons. Unlike fluorescence imaging, there is only one way of distributing probes, namely by delivering bioluminescent genes. Bioluminescence imaging reminds of fluorescent reporter gene imaging (e.g imaging of GFP) but has an advantage to this technique in that there is no intrinsic background. Since no excitation light is needed no autofluorescence can be stimulated in the tissue. Alike GFP imaging the optical reporter has been isolated from a light producing animals and plants.

3.2.1 Probes for bioluminescence imaging

The optical reporter in bioluminescence imaging is the Firefly luciferase gene. Inside a cell this gene encodes for an enzyme called Firefly luciferase. This enzyme is converted into luciferin by some chemical reactions, which emits photons when reacting with oxygen (figure 3.9).

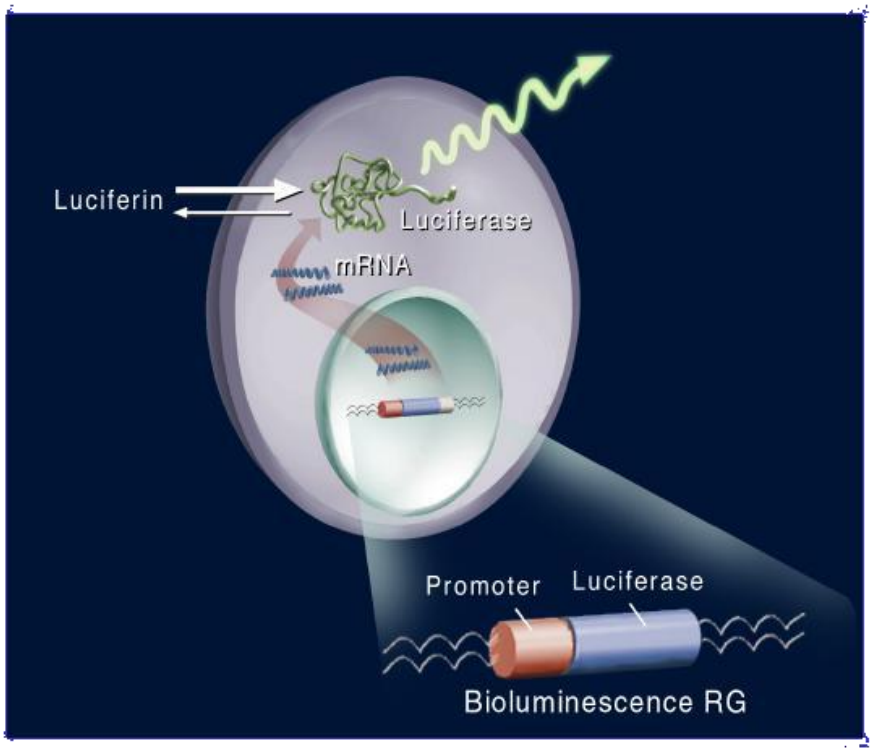

Figure 3.9. (Ref 7). A bioluminescent reporter gene delivered to a cell. The reporter gene encodes for a light emitting enzyme.

Firefly luciferin normally produces light at 562 nm but has in comparison with GFP been modified to produce red-shifted emission spectrum.
Bioluminescence imaging has been used for tracking tumor cells, stem cells and bacteria as well as for imaging gene expression[16].

Optical reporter gene imaging (i.e bioluminescence imaging and fluorescent reporter gene imaging) are suitable for molecular imaging in small animals, but are less likely to be adapted for clinical applications. The methods do neither allow absolute quantification of target signal. It is often used to follow disease progression in the same animal over time which can be seen in figure 3.10. For bioluminescence imaging the signal depends on ATP[f] (adenosine triphosphate), O_2 and depth.

[f] A phosphorylated nucleoside that supplies energy for many biochemical cellular processes.

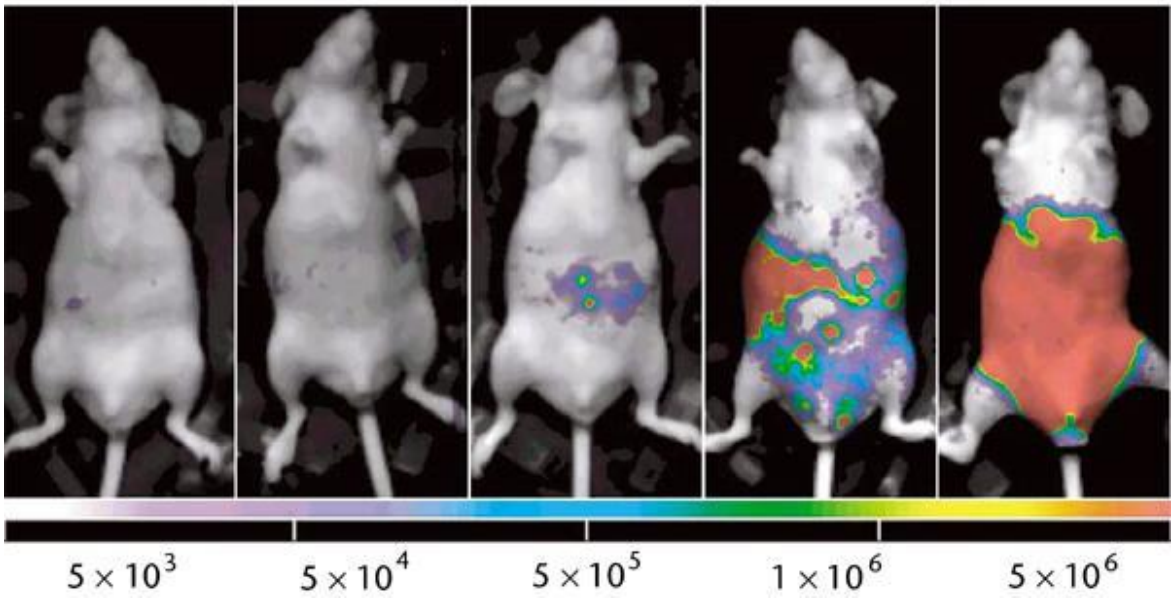

Figure 3.10. An example of imaging with bioluminescence. The picture shows a prostate cancer tumor modified with bioluminescent reporter genes. The growing of the cancer is imaged over time. The numbers below each image shows the number of bioluminescent cells. Reprinted from Ref 16.

3.3 Future outlook

Optical molecular imaging is an interesting field of molecular imaging due to the many advantages it provides: it is relatively cheap, non-radioactive and has many fields of application. However, to improve the method further, advances has to be made within several areas. The availability of more and further red-shifted probes must be improved. Such probes are important to minimize absorption, scattering and autofluorescence. New, activable and specific, probes must be engineered to extend the amount of targets possible to image. Making the measurements more quantitative is another important issue for optical imaging. This can be achieved with the use of photon migration theories. The lack of depth information (three dimensional) imaging is also a problem associated with optical imaging.

4 Theory of light interaction in tissue

When light interacts with tissue several processes can occur during the propagation through the medium. The various processes of absorption, scattering, reflectance, transmittance and fluorescence can be utilized for characterizing biological tissue. The interaction processes are strongly wavelength dependent. From an optical perspective, different types of tissue can be distinguished by the size and the shape of the cell, the distribution of absorbing substances, the scattering structures and any possible internal structure. Analyzing the propagation of light in tissue can yield information about optical properties; absorption and scattering coefficients μ_a and μ_s , and the scattering anisotropy factor or simply ‘‘g-factor’’. In section 4.1, the basic aspects of light-tissue interaction in simplified manner are presented.

When working with strongly scattering media, as in the case of tissue optical studies, you primarily have to deal with two problems, refered to as the *forward* problem and the *inverse* problem. Solving these problems is the key to calculate the lights distibution and the optical properties of the tissue[23,24].

The forward problem concerns the calculation of the energy density [Jm^{-3}] of the laser light in a certain position within the tissue, given that the optical absorption and scattering properties are known. The unknown optial properties of the inverse problem can be derived from measuring the distribution of reflected or transmitted light in the tissue[25].
The determination of the optical properties of tissue is a central part of tissue optics because in order to solve the inverse problem, the forward problem has to be solved first[26].

In other words, the fundamental problem is to describe how light propagates through biological tissue which consists of a large number of randomly distributed scattering kernels. The kernels may consist of small regions with a refractive index differing from the surrounding, as for example the mitochondria, cell membranes or even whole cells.
When both the forward and the inverse problem are solved, tissue optics can be a powerful tool within medical research. When the light propagation is accurately modeled and the scattering and absorption properties are quantified, tissue analysis can be used, for example, for diagnostic[27] purposes or for dose calculation[28] during laser treatment. In sections 4.2-4.3 this is further treated, along with different methods to model the propagation of light.

4.1 Light-tissue interaction

4.1.1 Light

The electromagnatic radiation spectrum stretches from wavelength less than 10^{-13} m to more than 10^{5} m. The visible light is composed of a narrow band of wavelengths between 400-780 nm.

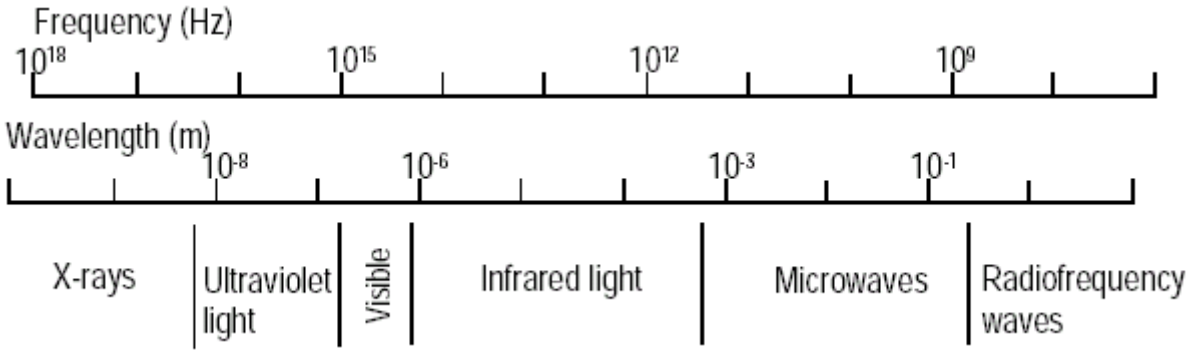

Fig. 4.1 The electromagnetic radiation spectrum.

The ultraviolet (UV) and the near infrared (NIR), bands are bordering this region. The wavelength (λ) of light, assumed to be well known, can be stated as:

$$\lambda = h \times \frac{c}{E} \qquad (7)$$

$$\nu = \frac{c}{\lambda} \qquad (8)$$

where *E* is the quanta of light energy, *v* is the frequency and *h* is Planck's constant.

4.1.2 Absorption

Biological tissue contains different absorbing molecules, chromophores, which absorbs energy in different wavelength regions. The absorption coefficient, μ_a [m^{-1}], describes the probability of the tissue molecules to absorb photons energy per unit length. The light absorption mainly depends on the type and the internal configuration of the molecules as well as their concentration and distribution within the tissue. The absorbed energy can be converted to heat, give rise to fluorescence or catalyze a photochemical reaction. Light in the UV region, below 400 nm, is strongly absorbed due to high concentration of absorbing molecules. Water, lipids and hemoglobin are the main absorbers in the visible and NIR region. Water is a dominant chromophore of most tissue above 900 nm with a peak around 970 nm. A wavelength region between approximately 700 – 1300 nm , often referred to as the optical window, is used for diagnostic and therapeutic purposes due to the deeper penetration into the tissue in this region. In this region, the blood absorption has decreased while the scattering coefficient is dominant[25].

4.1.3 Scattering

Light scattering is one of the most important processes that can occur during light propagation inside tissue. There are different contributors to light scattering in tissue. When the photon characteristics of light is applied, then light scattering is regarded on a molecular level. Photons may give rise to excitation process followed by de-excitation to either the initial state or to a higher/lower laying level. Relaxation to the initial state do not cause net energy transfer to the media, this means that the scattered photon still have the same wavelength as the incoming light (elastic scattering). However, relaxation to a higher/lower laying level implies a net change in the potential energy of the molecule. If the scattered photon has gained or lost energy a change in the wavelength has occurred (Raman scattering).

Light scattering from microscopic tissue components is hardly influencing the resultant of scattering characteristics. This is perceived at cellular and sub-cellular constituents, such as the cell membrane, organelles and cytoplasm[29]. The wave characteristics of light is almost exclusively applied when treating light scattering at microscopic level. Thus, light scattering is regarded as a process arising from spatial variations in refractive index. The refractive index of tissues varies in a very complicated manner at a microscopic level. Therefore a detailed description of the refractive index at this level is unfeasible. However, some important conclusions regarding light scattering on a microscopic level can be drawn. The main scattering features in tissue are the mitochondria[30] and lipid vesicles (fat droplets).

When applying the transport theory, a macroscopic refractive index is used due to the complexity of the microscopic structure. The macroscopic refractive index is measured by analyzing the Fresnel reflection from a tissue surface. The macroscopic refractive index of most tissue types measured in this way are in the range 1.38 – 1.41 at 632.8 nm[31].

4.1.4 Anisotropy factor

The scattering is assumed to be symmetric which means that the scattering phase function is a function of the scattering angle, such that $p(\mathbf{s},\mathbf{s}') = p(\theta)$, where θ is the angle between the incident and the scattered photon. It is further assumed that all photons have the same energy.

The **Henyey-Greenstein**[32] function is the analytical expression for the scattering phase function that is often used for light transport in biological tissue:

$$p(s,s') = p(\theta) = \frac{(1-g^2)}{2(1+g^2-2g\cos\theta)^{3/2}} \quad (4)$$

where g is the scattering anisotropy factor and is defined as $g = \langle\cos\theta\rangle$.

4.2 Ligth propagation models – the forward problem

It is possible to model the light scattering by two theories: wave theory (Maxwell's equations) or transport theory. The wave theory relies on solutions of the Maxwell equations which can be solved numerically. If we are investigating scattering from spherical particles, Mie theory is best suited[33,34], while T-matrix theory is the prime candidate to particles of arbitrary shape[38,39]. The optical properties are defined by the complex dielectric constant, $\varepsilon(\mathbf{r})$. The scattering and the absorption properties are represented by $\mathrm{Re}\{\varepsilon(\mathbf{r})\}$ and $\mathrm{Im}\{\varepsilon(\mathbf{r})\}$ respectively. However, the variation of $\varepsilon(\mathbf{r})$ on a microscopic level is vastly complex. Therefore, the transport theory is better suited for strongly scattering medium such as biological tissue.

In transport theory, the light propagation in tissue is treated as a stream of photons. Each photon transports a quantum of energy. The transport of the photons energy can mathematically be expressed by the radiative transport equation (RTE)[35,36].
The tissue is considered to be a homogeneous medium containing randomly distributed absorption and scattering centres, simply characterized by three parameters: the absorption and scattering coefficients, μ_a and μ_s, as well as the scattering anisotropy factor, g.

4.2.1 The transport equation

The radiative transport equation (RTE) has been very useful for calculating photon transport in tissue[37].
The equation treats the changes in the radiance ***L(r,s,t)*** **[$\mathbf{Wm^{-2}sr^{-1}}$]** which is the quantity that describes the propagation of photon power per unit area and unit solid angel in the direction **s**. The transport equation can be written as:

$$\frac{1}{c}\frac{\partial L(r,s,t)}{\partial t} = \\ = -s\cdot\nabla L(r,s,t) - (\mu_a + \mu_s)L(r,s,t) + \mu_s \int_{4\pi} L(r,s',t)p(s,s')d\omega' + Q(r,s,t) \qquad (1)$$

where c [m/s] is the speed of light in the medium, $\mu_a[m^{-1}]$ the absorption coefficient, $\mu_s[m^{-1}]$ the scattering coefficient, $p(\mathbf{s},\mathbf{s}')$ [-] the scattering phase function which gives the probability of scattering from direction $\mathbf{s}'$ into direction **s** and $d\omega(\mathbf{s})$ that denotes an infinitesimal solid angle in the direction **s**[23].
The change in number of photons, at position **r,** in direction **s** at time **t,** is represented in the left-side of equation (1). The first two terms of the right-side describe the amount of escaped photons over the volume boundary, and due to absorption and scattering into other directions, the third term describes gained photons due to scattering from other directions into **s** and the last term (Q) is the gain due to a light source inside the volume element.
The radiance can be stated as:

$$\boldsymbol{L(}\mathbf{r,s,t)} = \boldsymbol{N}(\mathbf{r,s,t)}\frac{hc^2}{\lambda} \qquad (2)$$

where $\boldsymbol{N}(\mathbf{r,s,t})$ [m^{-1} sr^{-1}] is the photon distribution function which is the volume density of photons per unit solid angle.

Another important quantity is the fluence rate Φ [W/m^2], which describes the power incident on a volume element per surface area:

$$\phi(r,t) = \int_{4\pi} L(r,s,t)d\omega(s) \qquad (3)$$

4.2.2 Solving the transport equation

Analytical solutions to the RTE are available only for a few special cases. On the other hand, there are various of methods based on approximation such as *diffusion approximation.* In practice, numerical methods such as *Adding-Doubling*[38] or *Monte Carlo*[39] simulations are the most widely used.
.

4.2.3 The Monte Carlo method

The conventional Monte Carlo method is frequently used as a model for simulating light transport in tissue. It is based on building a stochastic model where individual photons pathways are traced randomly. The scattering and absorption events are governed by the probabilities given by μ_s and μ_a as well as the phase function $p(\mathbf{s},\mathbf{s}')$.

One drawback with Monte Carlo simulations is the requirement of significant computation time if high precision and accuracy is wanted. It is also difficult to get good statistics if the point of interest is located far from the point of entry and the coefficients for absorption and scattering are high. However the method is a flexible and helpful tool for modelling and has no limitations concerning boundary conditions or spatial localization of inhomogeneities in the tissue.

The optical properties for each layer is defined before the simulation is started. Properties required are the absorption coefficient μ_a, the scattering coefficient μ_s , the anisotropy factor *g*, the refractive index *n* and thickness *d* of the sample. It is also necessary to define optical properties for the top ambient medium (most often air) and bottom ambient medium (if this is existent).

A number of photons, or rather photon packages, are launched into the medium. The number of photons used depends on which problem the simulation is supposed to solve. The reason for launching many photons at a time, as a packages, is that it improves the efficiency since normally only one photon follows the selected pathway. The packet starts off with a weight *w* set to 1. In several steps it has the possibility of being propagated undisturbed, absorbed, scattered, reflected internally or transmitted out of the tissue.

The simulation continues until the photon is either absorbed or exits the tissue. If it escapes the reflectance and transmission are recorded, and if it is absorbed the position where this took place is recorded. The final results from the simulation are fluence, transmittance, reflectance and photon absorption.

The program Monte Carlo simulation for Multi-Layered media, MCML, by Jacques and Wang[39,40], has become somewhat of a standard in the field of tissue optics.
An adaptation to time-resolved data and more complex geometries was implemented by Berg[41], but the photon propagation routines are the same for all subsequent versions of the program. Various Monte Carlo models were developed to simulate fluorescence spectra from layered tissues[42]. A basic approach to describe fluorescence within transport theory is to regard the propagation of the excitation light and the emission light as two different problems, and find a way to handle the transition of excitation light to fluorescence light.

4.3 The inverse problem

One of the more important aspects of the inverse problem is the number of the unknowns. There are spatial parameters, optical properties and also geometrical parameters, such as the thickness of the layer as unknowns. If the medium is homogeneous, the number of unknowns is reduced to the number of optical properties. Thus, the formulation to the inverse problem in such case is to find the optical properties μ_a, μ_s, and g, where the propagating light is measured.
There are two-parameters methods where both $\mu_s' = \mu_s(1-g)$ and μ_a are unknown and three parameters methods, where all three μ_s, μ_a and g are unknown such as the integrating sphere method[26], and the medium is assumed homogeneous.

4.3.1 Two-parameters methods

Two-parameters methods are based on measurements of the diffuse reflectance or transmittance from the medium. The measurements can be spatially resolved, time resolved or frequency resolved (see Fig. 4.2). Spatially resolved measurements are based on continuous wave (Cw) light. With this method, as well as with the time-resolved technique, it is possible to make measurements *in vivo*. The major advantage with the spatially resolved technique is that it can be performed with cheap light sources (*e.g.* lamps or diode lasers) and detectors (*e.g.* photodiodes). A drawback is that the method is sensitive to inhomogeneities in the medium[43].

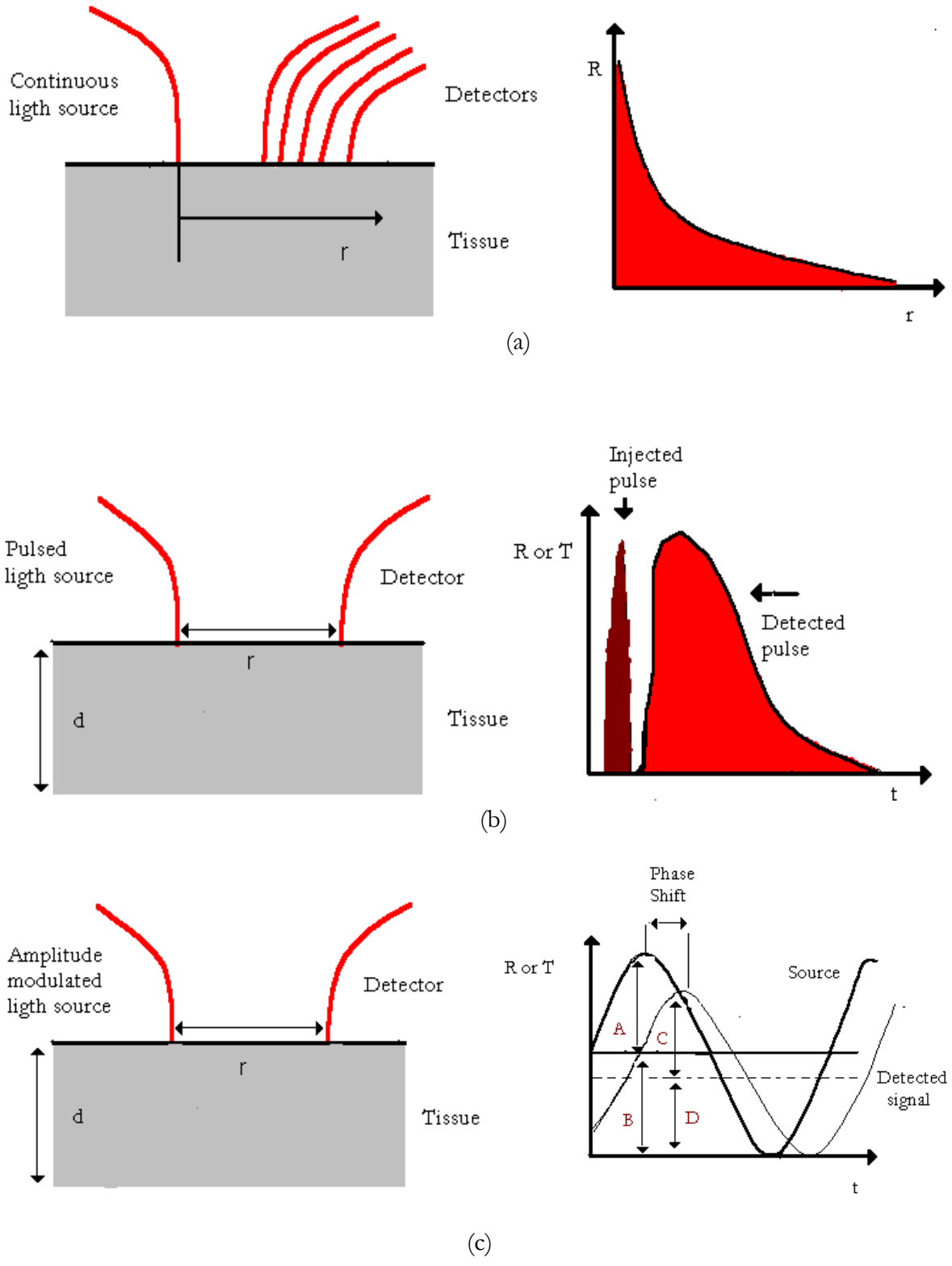

Fig.4.2 The principles of three two-parameters techniques to obtain μ_s' and μ_a, are schematically illustrated: (a) Cw spatially resolved reflectance measurement; (b) time resolved measurement and (c) frequency domain measurement where the phase shift and the modulation depth = BC/AD is measured.

4.3.2 The integrating sphere method

This method is used for measuring three parameters: collimated transmittance, I_{col} ,total transmittance, T_{meas}, and diffuse reflectance, R_{meas}. The optical parameters of the tissue are deduced from these measurements using different theoretical expressions and numerical methods to obtain μ_s ,μ_a and g.
The first parameter I_{col} is measured by letting a beam of light pass through a tissue sample and only measure the light that has not been scattered inside the tissue. This gives us the total interaction coefficient, $\mu_{t,meas} = \mu_a + \mu_s$. The total interaction coefficient can be recognised from the Beer-Lambert's formula, stating that the intensity of a beam passing straight through a sample with the thickness d decays exponentially:

$$I_{col} = I_0 \exp(-\mu_t . d) \qquad (5)$$

To measure the diffuse reflectance R_{meas} and the total transmittance, T_{meas}, a so called integrating sphere is used. Measuring T, the tissue sample is placed in front of the sphere. The light passes through the sample, is scattered and registered by a detector inside the sphere. The inside walls in the sphere are covered by a material that reflects the light in all directions. Measuring R the sample is placed in the end of the integrating sphere. The reflected light is collected in the sphere and detected.

Converting R,T and μ_t, to μ_a , μ_s and g are the solutions of an inverse problem. Polynomial regression is often recommended method. It is an iterative method which approximate the solutions to the forward model with 3-dimensional polynomials. A Monte Carlo generated database, producing maps of R_{MC} and T_{MC} as functions of μ_a , μ_s and g are used. An expansion of Chebychev polynomials is used to fit Monte Carlo generated data, yielding $R_{cheb}(\mu_a,\mu_s,g)$ and $T_{cheb}(\mu_a,\mu_s,g)$ (see figure 4.3). The optical properties are determined by finding the common roots of the new polynomials:

$$\begin{aligned} F(\mu_a,\mu_s,g) &= R_{cheb}(\mu_a,\mu_s,g) - R_{meas} \\ G(\mu_a,\mu_s,g) &= T_{cheb}(\mu_a,\mu_s,g) - T_{meas} \\ H(\mu_a,\mu_s,g) &= \mu_a + \mu_s - \mu_{t,meas} \end{aligned} \qquad (6)$$

The common roots is solved by setting the polynomial equal to zero which can be done by a Newton-Raphson solver.

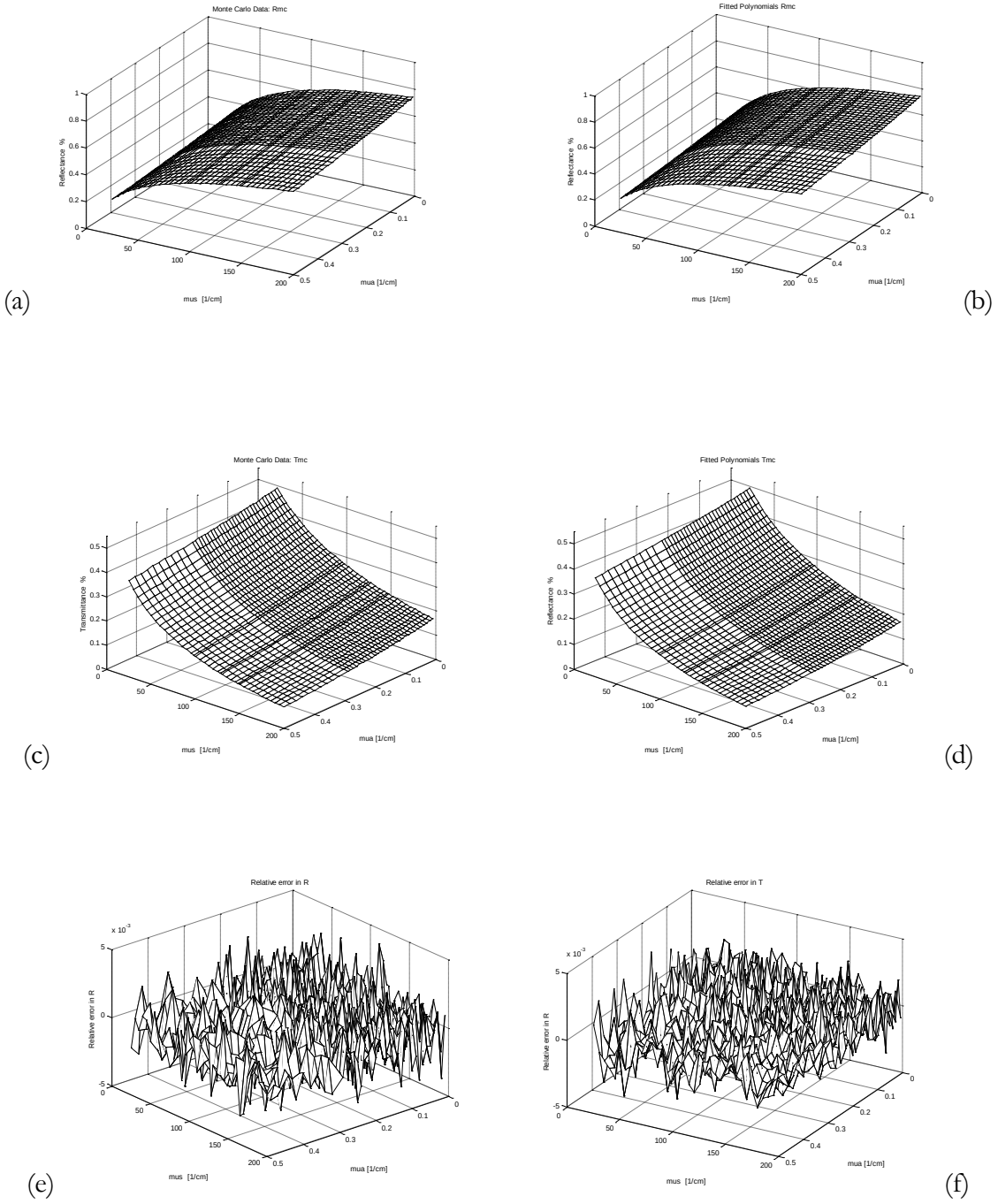

Fig.4.3 (a) and (c) show the Monte Carlo-computed data R_{MC} and T_{MC}. (b) and (d) show the corresponding fitted polynomials R_{cheb} and T_{cheb}. (e) and (f) show the relative error between the Monte Carlo data and the polynomials. Data are shown for g = 0.74.

5 Imaging deep interior tissue volumes

Much effort has been devoted to detect and image heterogeneities in biological tissues with diffuse near-infrared (NIR) light. Several investigators have been interested in the determination of the absorption and scattering coefficients in tissue and tissue-like phantoms. To enhance the specificity and sensitivity in tumor detection, fluorescent contrast agents have been frequently used. Several reconstruction algorithms have been published that attempt to recover the distribution of a fluorophore in a tissue volume given a set of measurements on the tissue surface. Fully three-dimensional reconstruction methods are being developed by some groups. Most commonly these are based on diffusion theory as the forward model[44,45], but an algorithm based on discrete-ordinates solution of the transport equation has also been proposed[46]. Many combinations of light source and detection points are needed for full reconstruction, which implies high complexity of both the instrumentation and the reconstruction algorithm. A simpler approach has been suggested by some authors, based on the approximation that the tissue can be regarded as a semi-infinite volume with fluorescing lesions at some depth from the surface. Stasic et al. presented a method based on the diffusion equation for a two-layer medium and spatially resolved measurements of both diffuse reflectance and fluorescence[47]. This method was successful in recovering the absorption and reduced scattering coefficients (μ_a and μ_s', respectively) of both layers, as well as the fluorophore concentration and depth of the layer. However, recovery of all parameters was limited to a depth of about 3 mm, and determination of the depth itself proved to be difficult for larger depths due to model coupling between depth, fluorophore concentration and tissue absorption. Eidsath et al. have described a method based on image fluorometry using a CCD camera[48]. Using a random-walk model, good accuracy of the determined depth was demonstrated for point-like fluorescing lesions.

6. Analysis of a fluorescence spectrum for determination of depth

The goal of the experimental part of this work is to develop a method for estimating the depth of fluorescent lesions in tissue. The method has been simulated on computer and compared with experimental results for validation.

The idea is to make use of changes in the spectral shape of the fluorescent light in order to reveal information about the depth. The changes are induced by tissue absorption and scattering as the light propagates from the fluorophore towards the surface of the body. Making use of the spectral properties of the fluorescent light is an alternative approach to those mentioned in section 5 (depth information) that not yet seem to have been investigated. To explain the idea, we consider a typical absorption/scattering spectrum of mammalian tissue (figure 6.1).

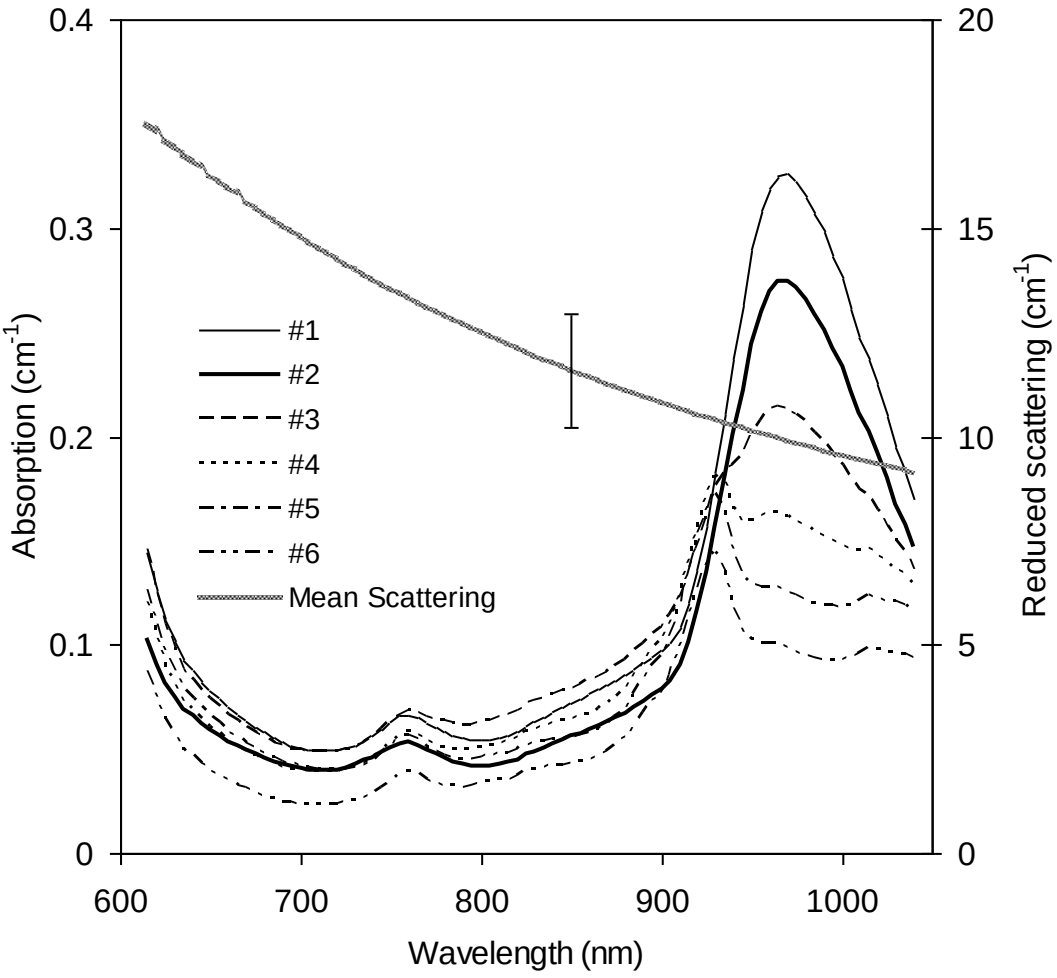

Figure 6.1. Optical properties of six different types of breast tissue[19]. The absorption spectra represent fitted data rather than actual measurements. The reduced scattering spectra were fitted to a power law. Only the mean spectrum is shown for scattering to avoid cluttering in the graph. The error bar indicates the standard deviation.

At around 600 nm a marked decrease in absorption can be observed. This is the beginning of the optical window. From 800 nm the absorption starts to increase slightly again, because of fat absorption and subsequently runs up just above 900 nm. The strong absorption around 970 nm is due to water in the tissue that has an absorption peak at this wavelength. Fluorescence light propagating through tissue with constant absorption and scattering would not have a change in the spectrum. The intensity of the fluorescence would decrease for longer pathways but the shape remains the same. However, a fluorophore whose emission spectrum covers a range where the absorption has a gradient (as around 600nm or above 900 nm) will have its fluorescence light altered in shape. Some of the emissions wavelengths will be absorbed more than others. This effect will be greater the longer the pathway through the tissue is. Our approach is to investigate whether the depth of a fluorophore embedded in tissue can be revealed from forming a ratio between two parts of the emission spectrum, affected by differently strong absorption. This is described by the simple formula:

$$\gamma = \frac{\Gamma(\lambda_1)}{\Gamma(\lambda_2)}$$

With data like those in figure 6.1 as template, computer simulations along with experimental phantom measurements were going to be made for different depths of fluorescent lesions in order to investigate whether the spectral changes can be used to reveal the depth. In the simulations $\Gamma(\lambda)$ represents the probability of detecting a photon of wavelength λ at the surface of the sample, and in the experimental measurements $\Gamma(\lambda)$ is the measured intensity at the surface of the phantom of the detected light at wavelength λ.

In addition to absorption - scattering and the measurement geometry will affect the deformation of the fluorescent spectra. This is also taken into account in the simulations.

7 Material and method

Performing simulations of a fluorescent lesion on different depths in tissue is rather unproblematic. The programs available request information about the optical properties of the tissue, at the wavelength of the excitation and fluorescence light along with the shape and size of the sample. Most questions raised during this work therefore regard the practical part of the experiments, i.e. the phantom measurements.

Before and during the measurements and simulations the following issues are necessary to be considered:

- Which tissue optical properties that should be used as model for the simulations and phantom measurements
- The best possible wavelength range for this type of measurements
- Choosing of fluorescent dye
- Excitation source
- Type of phantom
- Which detector to use
- Method of simulation
- Convenient quotient

At the department of Atom Physics in Lund, previous measurements of breast tissue have been made. The access to those and the fact that optical imaging and breast cancer research often are linked together makes it appropriate to use these data. The absorption/scattering spectra of six different types of breast tissue are shown in figure 6.1. A fluorescent dye in this, red, spectral region seldom fluoresces over a bandwidth greater than 200 nm[42]. In the graph shown in figure 5.1 there are two regions of non-uniform absorption likely to give rise to measurable changes in the relative spectral intensity of the fluorescence light. These two regions where the absorption changes dramatically are as mentioned earlier around 600 nm and just above 900nm. Since no fluorescence will cover them both, one has to be chosen. One advantage with the latter is that the absorption is low for shorter wavelengths than 900nm, where the dye will have its absorption maximum. This implies greater penetration depth for the excitation light. A fluorophore that emits at, for example, 620nm has its absorption peak around 560 nm. At this wavelength the tissue is much less transparent and the light exciting the dye would not reach deep into the tissue. Another advantage is that the dominant absorbers in tissue at wavelengths above 900 nm are water and lipids, which facilitate the preparation of a liquid phantom with well agreeing optical tissue properties for the region of interest. Below 600 nm, on the contrary, the absorption is caused by deoxygenated and oxygenated hemoglobin. With this motivation the region above 900nm was decided to be used for the experiments. Next a fluorophore emitting light in this spectral area along with a suitable excitation source and detector had to be found. The best available excitation source in the NIR region was a Ti:Sapphire laser at 780 nm. Having decided the excitation laser light source reduced the amount of usable fluorescent dyes severely. The excitation wavelength of

the laser and the absorption maximum should match in order to get as much light as possible out from the dye. Two fluorescent dyes remained that had absorption maximum around 780nm and could be used for lasing up to 1000nm. Those were IR-140 (Exciton, USA) and LC9280 (Lambda Physik, Germany). Since laser dyes in the NIR region have very poor solubility in water and poor quantum yield we decided to try them both to increase the chances of good results.

During the experiments three different detectors were tried out. All but one showed way to high signal-to-noise ratio of the detected fluorescence at the surface of the phantom. The first one investigated was a STREAK camera operating in the NIR region which not only provides spectral but also temporal information. The temporal information was meant to be compared with the spectral to demonstrate advantages of using spectrally resolved measurements or, alternatively, to gain additional information about the depth. The STREAK camera had far too low sensitivity and required hours of detection time already at relatively shallow tumor depth. The second detector was a non-cooled spectrometer (Princeton Instruments) with fairly good sensitivity in the NIR spectrum. With this detector the detection time was reduced but the signal-to-noise ratio was higher than what could be accepted. The final detector was far more sensitive for the measurements than the other two. This detector (HoloSpec f/1.8i, Kaiser Optical Systems, USA) consists of a spectrometer and a cooled CCD camera coupled together. It is normally used for RAMAN spectroscopy in the region around 900nm.

(We use Monte Carlo simulations to compute fluorescence spectra. The Monte Carlo code was developed earlier and is especially suited for simulating fluorescence from layered tissue[42].)

7.1 MC-simulations

For experimental validation we performed Monte Carlo simulations with optical properties similar to phantoms, whose optical properties were measured independently using an integrating-sphere method (sections 7.2.1 and 7.2.2 below).
The amount of traced photons were 5×10^5. All other values (e.g. excitation wavelength, distance between detection point and excitation point) were in correspondence with the experimental phantom measurements.

7.2 Tissue phantom

Measurements were performed on a model that consisted of three parts: the upper and the lower parts, where the liquid phantom material was stored, and in between those a 1 mm thick layer, where the same liquid with some added fluorescent dye was kept see figure 7.1. The walls of the model was made of two plastic cylinders (∅=7cm). In the bottom of each cylinder, thin plastic film was attached, for separating the liquids without affecting the light when propagating between them. The third layer was constructed by placing the two cylinders on top of each other, with their film–covered surfaces facing each other and isolating the small resulting volume. Liquid could easily be added and removed to the upper part so the height of the surface could be varied (i.e the depth of the fluorophore), see figure 7.1.

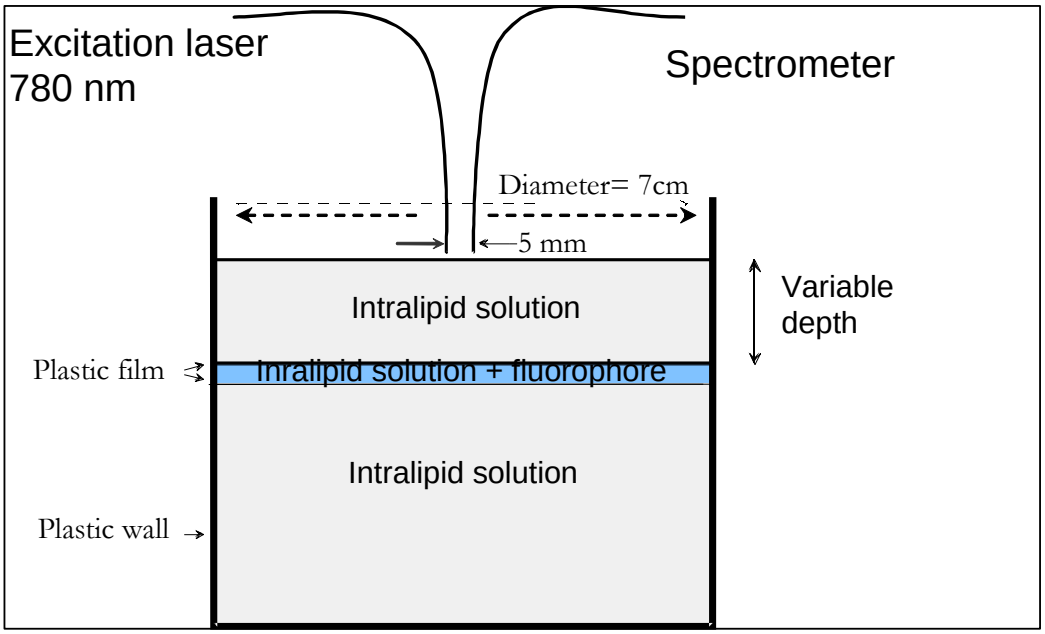

Figure 7.1. Water based tissue phantom with variable depth of the fluorescent lesion.

7.2.1 Preparing the liquid phantom

The liquid tissue phantom was prepared by mixing 21 parts of water with 1 part 20%-Intra lipid® solution (Fresenius Kabi AG) which corresponds to a lipid concentration of 0.91%. To increase the absorption a concentration of 2.3 µl ink/liter was added to the lipid mix. Figure A.1 (Appendix 1) describes how the overall absorption varies as a function of different amount of added ink. 2.3 µl ink/liter puts the absorption on a level very proximate to the template values. The black ink was taken from a copying machine. Resulting absorption and scattering properties were measured with an integrating sphere. To translate R and T to μ_a , μ_s and μ_s' a Monte Carlo database was generated specifically designed for this application (section 4.3.2). The generated database covered an interval of 1 to 200 cm^{-1} and 0.01-0.4 cm^{-1} for μ_s' and μ_a respectively.

The absorption and scattering properties of the liquid as a function of wavelength are presented in figure 8.3 below. The prepared Intra lipid® solution simulates healthy tissue and was kept in the upper and the lower part of the beacon, see figure 7.1.

7.2.2 Fluorescent layer

For the intermediate layer of the phantom a solution with the same optical properties as the rest of the phantom, but with fluorescent properties had to be prepared. This was achieved simply by adding a small amount of dye solved in ethanol to the 0.91% Intra lipid® solution. The amount of dye solution should be as high as possible in order to maximize the fluorescence but low enough not to affect the optical properties in the spectral region where the measurement were going to be made. The main concern was that the dye would absorb above 870 nm and in such manner disturb the measurements by reabsorbing its fluorescence. By pointwise integrating sphere measurements, using interference filter, the highest possible

concentration was found. Such measurements were made for the two available dyes, IR-140 and LC9280. It appeared to be possible to add more than twice as much LC9280 to the solution as IR-140. However, the strength of the fluorescence were almost similar for the two dyes so nothing was gained by the possibility to use the higher concentration LC9280 solution. On the contrary, the higher amount of alcoholic solution was more of a drawback since the intralipid showed tendencies to aggregate rather quickly. The conclusion was that IR-140 was a more efficient dye than LC9280 and was therefore used for the rest of the measurements.

In appendix 2 pointwise integrating sphere measurements of dye/Intra lipid® mix is presented.

7.3 Experimental phantom measurement

Figure 7.2 illustrates the experimental arrangement used for the measurements. Two fibers (Super Guide, ∅ = 400 μm, NA = 0.22; Fiberguide Industries) were led into the upper part of the phantom, one for the excitation light and one for detection of fluorescence. The light from the laser passed an interference filter of 780 nm (filter 1) before entering the fiber and had an intensity of approximately 10mW when illuminating the surface of the phantom. The detection light was filtered with long-pass filter (RG 780; Schott Glass Technologies, Inc.), filter 2, to ensure no back scattered light from the excitation light was mixed with the fluorescence light. The light was led into a holographic imaging spectrograph (HoloSpec f/1.8i; Kaiser Optical Systems, Inc.) with an interference grating efficacious from 815nm to 960nm. A nitrogen-cooled CCD camera (LN/CCD-1024-EERB/1; Princeton Instruments, Inc.) recorded the spectral image. The CCD was coupled to a detector controller (Princeton Instruments, Inc) and was set to operate at a temperature of -110°C. To view the resulting spectrum and to communicate with the CCD the program WinSpec/32 version 2.3.3.3 (Roper Scientific, Inc.) was used.

(The excitation light was led out from the oscillator of the tera-watt laser at Lund Laser Centre. This is a pulsed Ti:Sapphire laser pumped with an Ar^+ -laser. After passing the 780nm interference filter the pulse was strongly broadened, but in our experiment temporal information was not of interest.)

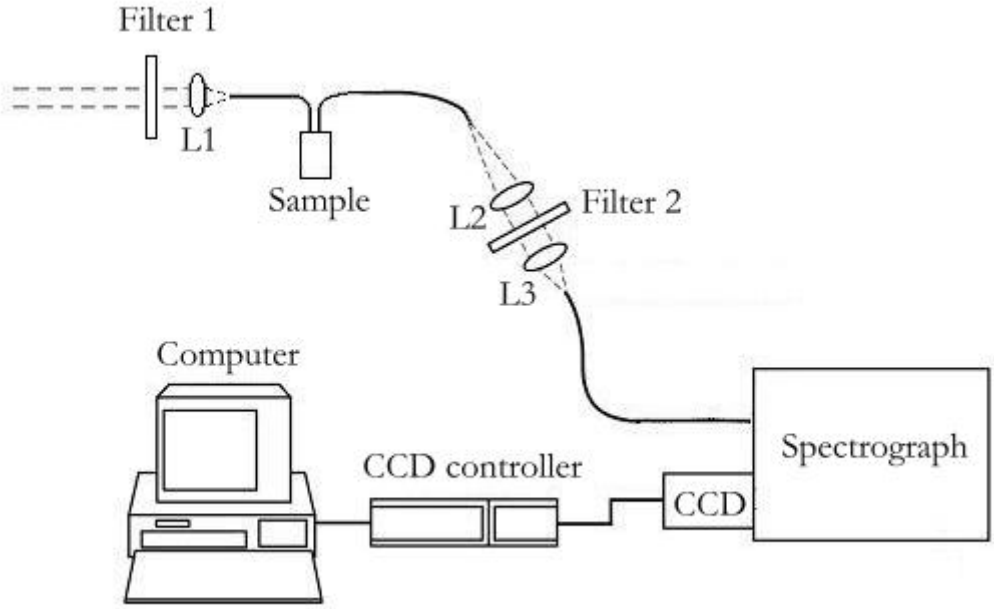

Figure 7.2 Schematic diagram of the set-up for spectroscopy measurements.

During measurements the height of the liquid tissue material was increased by 1.14 mm at a time, starting from 0mm to 1.14cm. Spectra were acquired in the wavelength range of 815-960 nm.

8 Results

The optical properties of the Intralipid phantom as determined by the integrating sphere method (shown in fig. 8.1) were used as input for the Monte Carlo simulations.

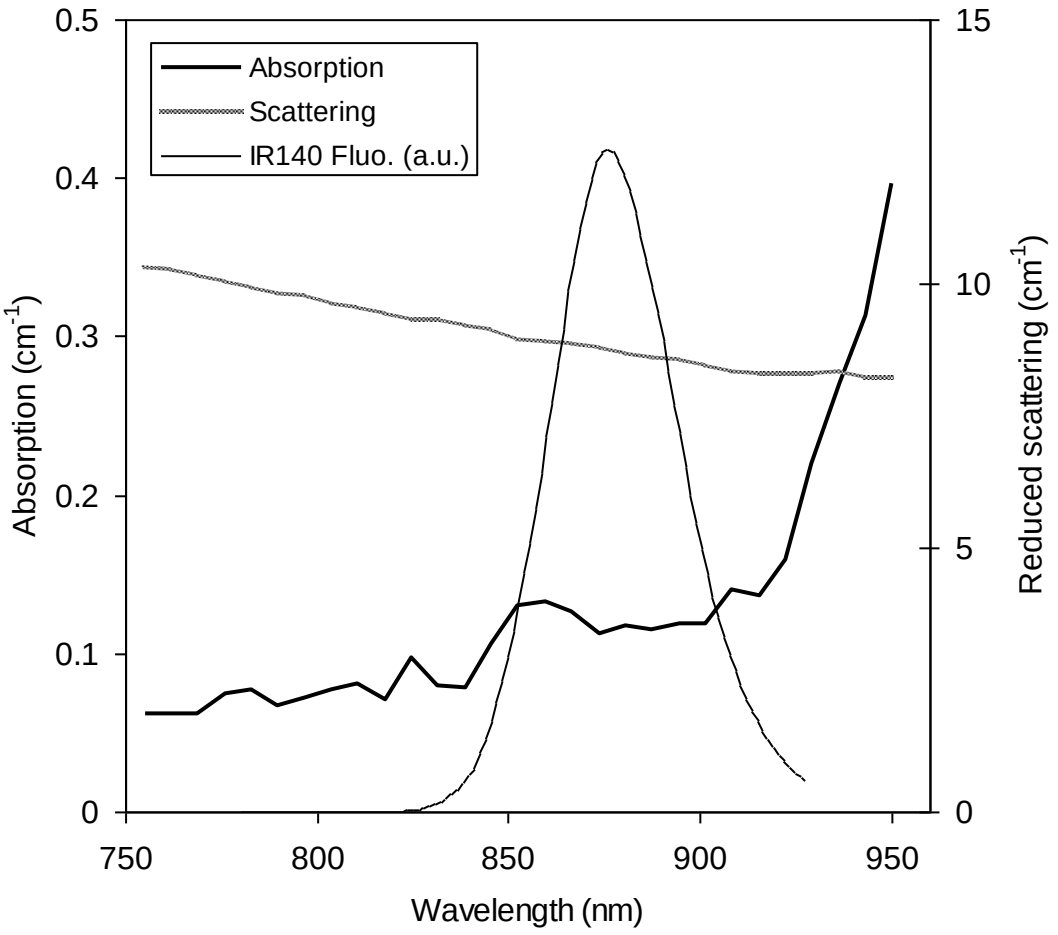

Figure 8.1. The optical properties of the Intra lipid phantom. The intrinsic fluorescence spectrum of IR-140 is also shown.

In this case g was around 0.65 over the wavelength range. The measured fluorescence spectra at different depths are presented in figure 6.4, which shows the shift of the spectrum as the depth increases.

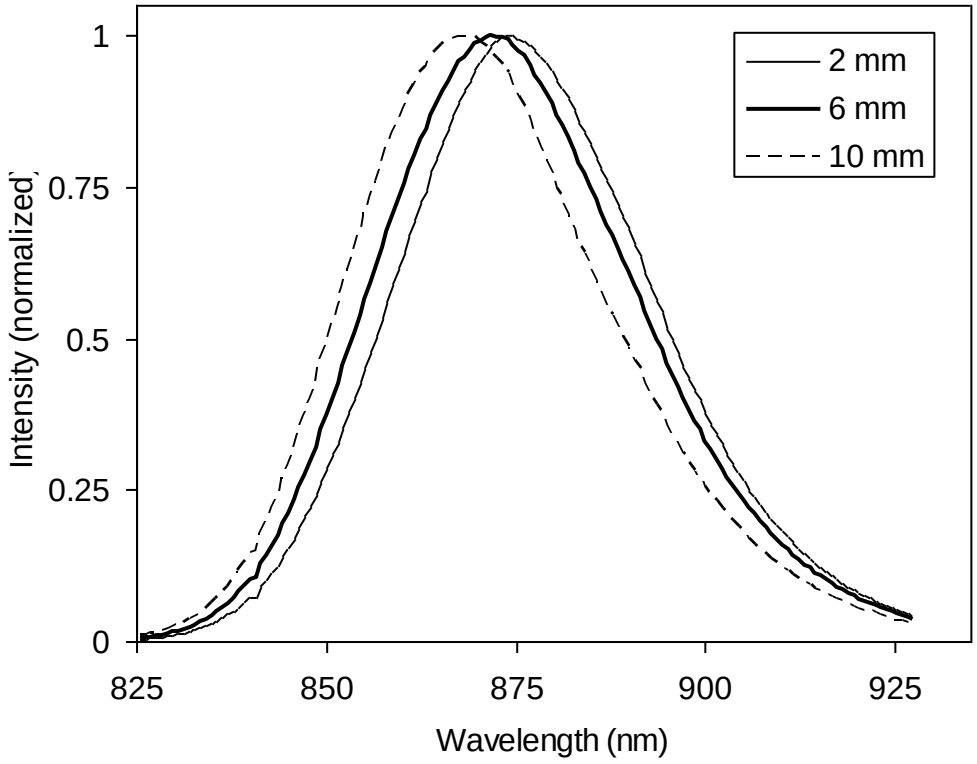

Figure 8.2 Measured (normalized) fluorscence spectra for different depths of the layer with fluorescing IR 140: 2, 6 and 10 mm.

In the Monte Carlo simulations, the highest value of the ratio γ was obtained with λ_1=815 nm and λ_2=960 nm. However, due to the low fluorescence signal at long wavelengths we had to use a lower λ_2 to obtain a good signal-to-noise ratio from the measurements. Due to influence of autofluorescence when the excitation and detection fibers were close together we used a fiber distance of 5 mm. Therefore, the measurement was limited to depths larger than about 1 mm. In figure 6.5 we present γ (normalized to the value at d=2 mm) as a function of d for λ_1=886 nm and λ_2=922 nm.

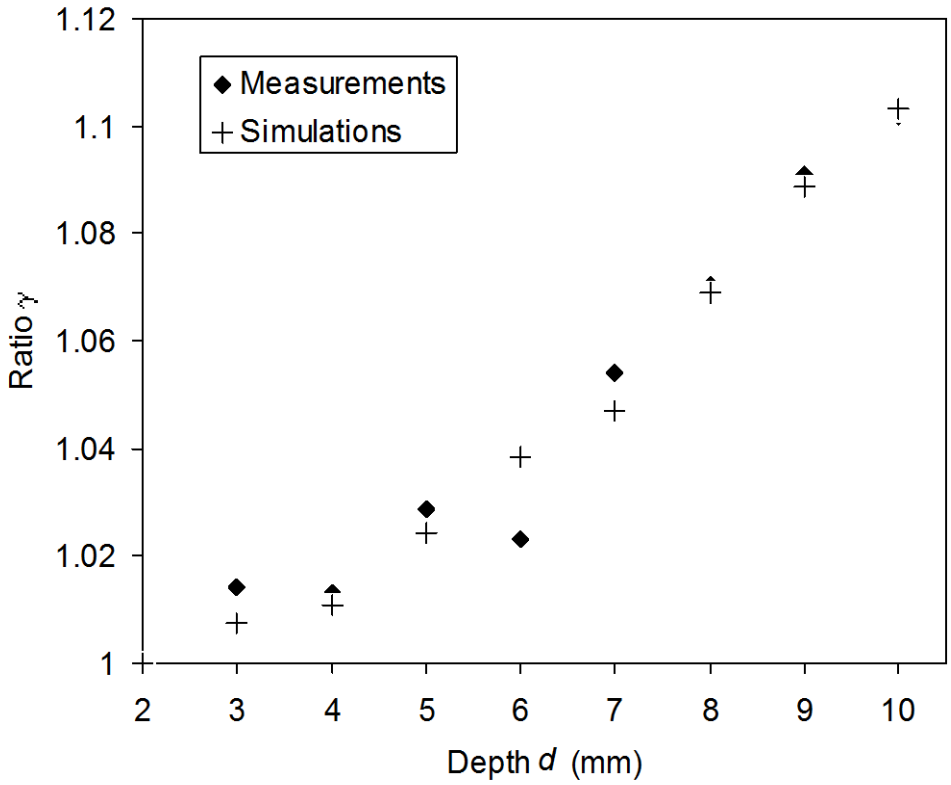

Figure 8.3. The ratio γ shown for λ_1 = 886 nm and λ_2 = 922 nm, as a function of the depth *d*, normalized to the value for *d*=2. Results from both measurements on the Intralipid phantom and the Monte Carlo simulations are shown.

9 Discussion and Conclusions

The results from the Monte Carlo simulations show that the ratio $\gamma(\lambda_1,\lambda_2)$ indeed is a useful indicator of the depth of a fluorescing lesion for the right combinations of wavelengths λ_1 and λ_2. The results from the phantom measurements corroborate the simulations and show that the method is practically feasible using a relatively simple experimental set-up. In the case of the Intralipid phantom we utilize the difference in water absorption that has a maximum absorption at 970 nm. Here we used λ_2=922 nm, although a longer wavelength would have given a higher ratio γ, but we were limited to about 930 nm by the spectrometer and the fact that the fluorescence spectrum for IR-140 drops to low intensity for longer wavelengths (as can be seen in figure 6.3). It is worth to mention that the amount of dyes fluorescing above 850 nm is rather limited. An alternative to IR-140 and LC9280, that fluoresce farther up in the NIR region, but still have good absorption around 780 nm would be ideal. A more careful analysis of the results show that we were able to recover the depth of the fluorescing layer from the experimental data with an accuracy of 0.6 mm[42].

A better choice of wavelengths would be (λ_1,λ_2)=(875 nm,935 nm). With this pair of wavelengths it has been shown in ref 50, that the depth can be recovered with good accuracy and small dependence on variations in breast tissue from one person to another. This study, however, is not conducted within this master thesis. To change region to the slope at 600-650 nm could also be an interesting idea.

With the present method, we envision a potential application based on a probe delivering excitation light and at the same time detecting the fluorescence light by means of relatively simple photodetectors and wavelength-selecting filters. The operator would manually scan the probe across the tissue and information would be presented in the form of an indicator of fluorescence intensity and the estimated depth of the fluorophore. We also consider our method very promising in terms of providing depth information for image fluorometry and molecular imaging, as a means to resolve the fluorophore distribution in three dimensions[22].

Acknowledgements

We would like to thank our supervisors, Jenny Svensson and Stefan Andersson-Engels, for their guidance and encouragement, making this thesis possible. We would also like to express our sincere gratitude to Johannes Swartling, for his support and work with the published article, Christoffer Abrahamsson, for technical help during the experimental measurements and Nazila Yavari for her engagement in needed situations.

Finally, we would like to thank our families and friends for all backing support.

Khaled Terike and Daniel Bengtsson

References

1. Tarik F. Massoud, Sanjiv S. Gambhir,"Molecular imaging in living subjects: seeing fundamental biological processes in a new light," Genes and development **17**, 545-580, (2003).

2. Bogdanov A, Weissleder R., "The development of in vivo imaging systems to study gene expression," Trends Biotechnol 16,5-10, (1998).

3. Christoph Bremer, Ralph Weissleder, "In vivo imaging of gene expression: MR and optical technologies," Acad Radiol 8,15-23, (2001).

4. Robert F. Service, "New probes open windows on gene expression, and more," Science 280, 15 may (1998).

5. Roush, W., "Antisence Aims for a Renaissance," Science 276, 1192-1193, (1997)

6. Bremer C, Bredow S, Mahmood U, Weissleder R, Tung C-H, "Optical imaging of matrix metalloproteinase-2 activity in tumors: feasibility study in a mouse model," Radiology 221,523-529, (2001).

7. Crump institute for molecular imaging, "Lecture on Molecular Imaging", http://laxmi.nuc.ucla.edu:8248/M248_04/syllabus.html (2004).

8. Weissleder R, "Scaling down imaging: Molecular mapping of cancer in mice," Nat. Rev. Cancer 2, 11-18, (2002).

9. Ching-Hsuan Tung et al., "In vivo imaging of proteolytic enzyme activity using a novel molecular reporter," Cancer research 60, 4953-4958, September (2000).

10. Molecular probes, Inc., Haugland, R.P. , "*Molecular Probes Handbook for Fluorescent Probes and Research Chemicals*, 6th Edition" http://www.probes.com (1996).

11. Imaging research, Inc., "Fluorescence imaging," http://www.imagingresearch.com/applications/Fluorescence.asp (2004).

12. Brackmann, U. "Lambdachrome laser dyes," Lambda Physik, Göttingen 2000 (3rd edition)

13. Lin et al, "Novel Near-Infrared Cyanine Fluorochromes: synthesis, Properties, and Bioconjugation," Biocon Chem 13, 605-610, (2002).

14. Mitchell, P, "Turning the spotlight on cellular imaging," *Nat Biotechnol* **19**,1013-1017, (2001).

15. Bremer et al, "Imaging of Differential Protease Expression in Breast Cancers for Detection of Aggressive Tumor Phenotypes," *Radiology* 222,814-818, (2002).

16. Weissleder, R. Ntziachristos, V. "Shedding light onto live molecular targets," Nature medicine 9(1), 123-128, January (2003).

17. Evident Technologies, Inc. "Quantum dots explained," http://www.evidenttech.com/qdot-definition/quantum-dot-about.php

18. Benoit Dubertret et al.**"** In Vivo Imaging of Quantum Dots Encapsulated in Phospholipid Micelles," Science vol 298, 29 november 2002 1759-1762

19. A. Pifferi, J. Swartling, E. Chikoidze, A. Torricelli, P. Taroni, A. Bassi, S. Andersson-Engels, and R. Cubeddu, "Spectroscopic time-resolved diffuse reflectance and transmittance

20. Molecular probes, Inc., "*Molecular Probes Handbook for Fluorescent Probes and Research Chemicals*," http://www.probes.com/handbook/figures/0665.html

21. Swartling et al, "Fluorescence spectra provide information on the depth of fluorescent lesions in tissue"

22. C. Bremer, V. Ntziachristos, R. Weissleder, "Optical-based molecular imaging: contrast agents and potential medical applications," Eur. Radiol. 13, 231-243 (2003)

23. A. Ishimaru, *Wave propagation and scattering in random media* (Academic press, New York, 1978).

24. K. M. Case and P. F. Zweifel, *Linear transport theory* (Addison-Wesley Publishing Co. 1967).

25. W. F. Cheong, S. A. Prahl, and A. J. Welch, "*A review of the optical properties of biological tissues*," IEEE J. Quant. Electr. **26,** 2166-2185 (1990).

26. J.Swartling, *Biomedical and atmospheric applications of optical spectroscopy scattering media*, (2002). Ph.D. Thesis, Lund Institute Technology, Lund, Sweden.

27. R. Splinter, R. H. Svenson, L. Littman, J. R. Tuntelder, C. H. Chuang, G. P. Tatsis, and M. Thompson, *"Optical properties of normal, diseased, and laser photocoagulated myocardium at the Nd:YAG wavelength,"* Lasers Surg. Med. **11,** 117-124 (1991).

28. R. Berg, "Laser-based cancer diagnostics and therapy- Tissue optics considerations" (1995). Ph. D. Thesis, Lund Institute of Technology, Lund, Sweden.

29. A. M. K. Enejder, "Light scattering and absorption in tissue- models and measurements," (1997). Ph.D. Thesis, Lund Institute of Technology, Lund, Sweden.

30. B. Deauvoit, S. M. Evans, T. W. Jenkins, E. E. Miller, nad B. Chance, " Correlation between the light scattering and the mitochondrial content of normal tissues and transplantable rodent tumors," Anal. Biochem. **226**, 167-174 (1995).

31. F. B. Bolin, L.E. Preuss, R. C. Tayler, and R. J. Ference, " Refractive index of some mammalian tissue using a fiber optic cladding method," Appl. Opt. **28**, 2297-2303 (1998).

32. L. G. Henyey and J. L. Greenstein, " Diffuse Radiation in the galaxy," Astrophys. J. **93**, 73-83 (1941).

33. C. F. Bohren and D. R. Huffman, *Absorption and scattering of light by small particles* (John Wiley & Sons, Inc. New York, 1983).

34. H. C. van de Hulst, *Light scattering by small particles* (Wiley, New York, 1957).

35. A. Ishimaru, *Wave propagation and scattering in random media* (Academic press, New York, 1978).

36. K. M. Case and P. F. Zweifel, *Linear transport theory* (Addison-Wesley Publishing Co. 1967).

37. K. M. Case, "Elementary solutions of the transport equation and their applications," Annals of Physics **9,** 1-23 (1960).

38. S. A. Prahl, M. J. C. van Gemert, and A. J. Welch, "Determining the optical properties of turbid media by using the adding-doubling method," Appl. Opt. **32,** 559-568 (1993).

39. S. A. Prahl, M. Keijzer, S. L. Jacques and A. J.Welch, *A Monte Carlo Model of Light Propagation in Tissue*, SPIE Institute Series Vol IS 5, 1989

40. L. Wang and S. L. Jacques, *Monte Carlo Modeling of Light Transport in Multi-layeredTissues in Standard C,* 1992

41. R. Berg, "Laser-based cancer diagnostics and therapy- Tissue optics considerations" (1995). Ph. D. Thesis, Lund Institute of Technology, Lund, Sweden.

42. J. Swartling, A.Pifferi, A:M:K:Enejder, and S.Andersson_Engels, "Accelerated Monte Carlo model to simulate fluorescence spectra from layered tissues," Journal of the Optical Society of America, in press (2002).

43. Daniel J. Hawrysz and Eva M. Sevick-Muraka, " Development Toward Diagnostic Breast Cancer Imaging Using Near_Infrared Optical Measurenents and Fluorescent Contrast Agents". Neoplasia, Vol. 2. No. 5, September- October, 2000, pp. 388-417.

44. M.J. Eppstein, D.J. Hawrysz, A. Godavarty, and E.M. Sevick-Muraca, "Three-dimensional, Bayesian image reconstruction from sparse and noisy data sets: near-infrared fluorescence tomography," Proc.Natl.Acad.Sci. 99, 9619-9624 (2002)

45. A.B. Milstein, S. Oh, K.J. Webb, C.A. Bouman, Q. Zhang, D.A. Boas, and R.P. Millane, "Fluorescence optical diffusion tomography," Appl.Opt. 42, 3081-3094 (2004)

46. A. D. Klose, A. H. Hielscher, "Fluorescence tomography with simulated data based on the equation of radiative transfer," Opt. Lett. 28, 1019-1021 (2003)

47. D. Stasic, T.J. Farrell, and M.S. Patterson, "The use of spatially-resolved fluorescence and reflectance to determine interface depth in layered fluorophore distributions," Phys.Med.Biol. 48, 3459-3474 (2003)

48. A. Eidsath, V. Chernomordik, A.H. Gandjbakhche, P. Smith, and A. Russo, "Three-dimensional localization of fluorescent masses deeply embedded in tissue," Phys.Med.Biol. 47, 4079-4092 (2002)

49. Pifferi, A. Swartling, J. Chikoidze, E. Torricelli, A. Taroni, P. Bassi, A. Andersson-Engels, S. and Cubeddu, R. "Spectroscopic time-resolved diffuse reflectance and

50. Swartling, J. Svensson, J. Bengtsson, D. Terike, K. Andersson-Engels, S. "Fluorescence spectra provide information on the
depth of fluorescent lesions in tissue"

Appendix 1

Absorption of the phantom liquid as a function of added ink

Five samples with different concentration of ink were prepared and absorption measurements were performed with an integrating sphere. The measurements were conducted by first preparing two premix solutions, one of ink and one of pure 0,91% Intralipid solution. These two premixes were mixed in five different amounts that were separately measured with the integrating sphere. Figure A.1 shows these five measurements for all wavelenghts, and in figure A.2 the linear relationship between the five measuremetns is shown. The following concentrations were prepared:

Premix of Intralipid (1): 600 microliter Intralipid + 21*600 microliter water, eg 0,91 % Intralipid solution.
Premix of Ink solution (2) : 13200 micro liter of premix (1) is mixed with 4 micro liter ink resulting in 3,029385*10^-4 micro liter ink/micro liter solution.

Five samples of premix (1) is mixed with different amount of premix (2) in the following concentrations:

1. 0,22932 micro liter ink / liter solution
2. 2,27773 micro liter ink / liter solution
3. 4,52147 micro liter ink / liter solution
4. 6,73196 micro liter ink / liter solution
5. 8,90995 micro liter ink / liter solution

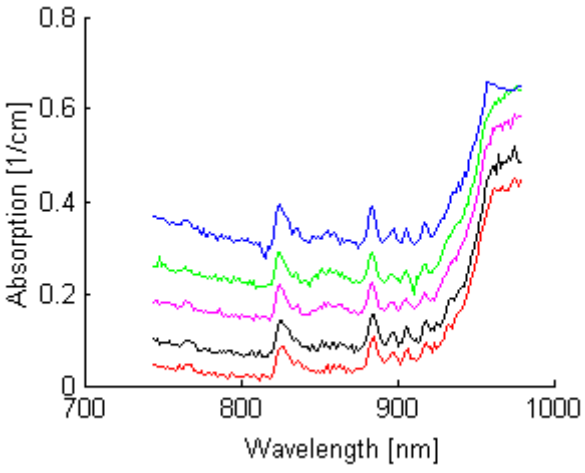

Figure A.1 The absorption coefficient for different amount of added inc to the Intralipid solution.

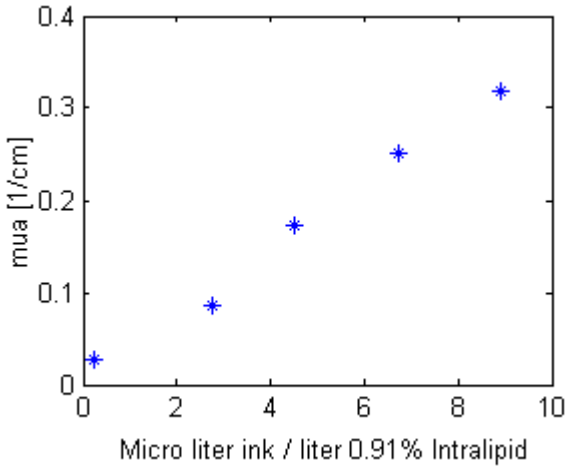

Figure A.2. Absorption as a function of ink concentration, wavelength = 850 nm.

Appendix 2

Through pointwise absorption measurements with interference filter the highest dye concentration, not affecting the overall absorption after 870 nm, can be decided. The measurement in figure A.3 is of a concentration of IR-140 that was used later during the following phantom measurements.

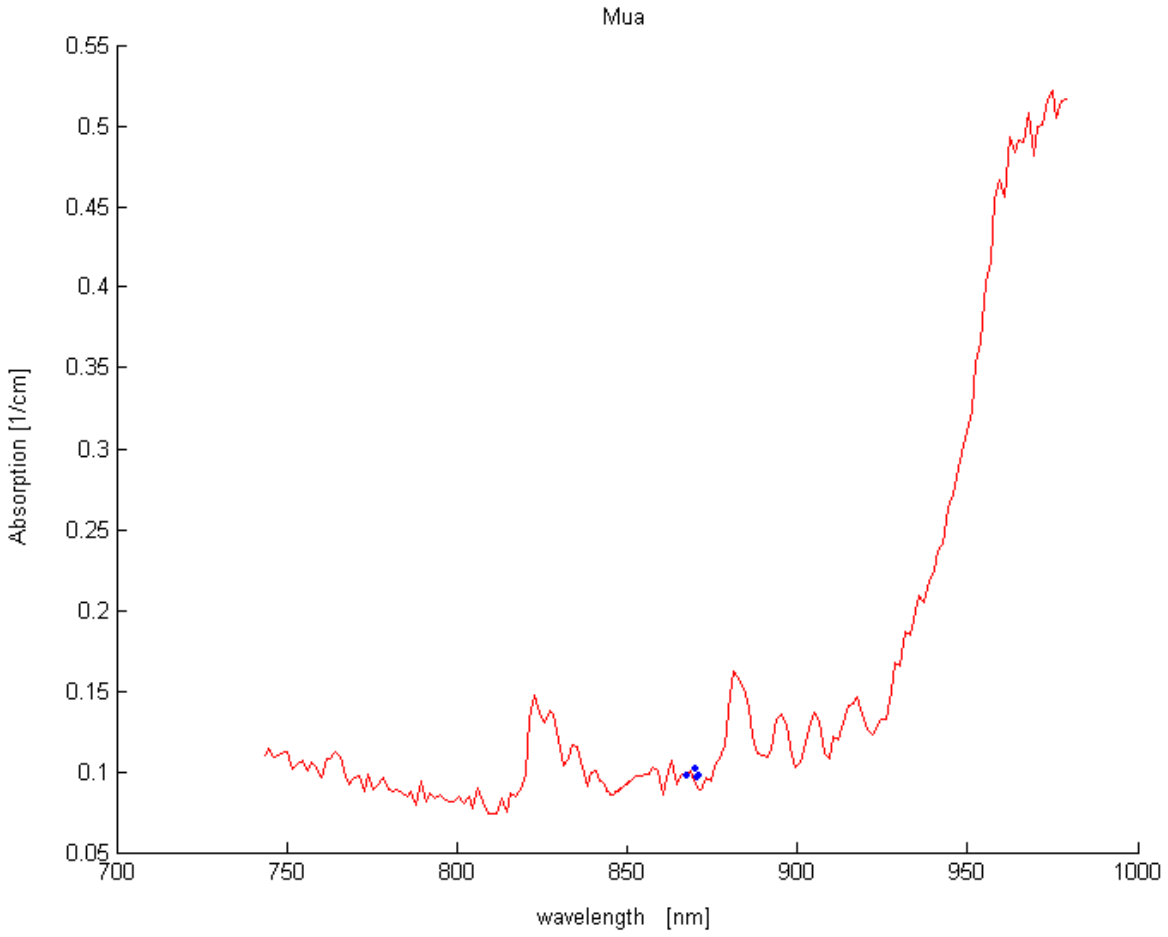

Figure A.3 Pointwise integrating sphere maesurements using filter at wavelength 870 nm.